

Studies of jet quenching using isolated-photon+jet correlations in PbPb and pp collisions at $\sqrt{s_{NN}} = 2.76$ TeV

The CMS Collaboration*

Abstract

Results from the first study of isolated-photon+jet correlations in relativistic heavy ion collisions are reported. The analysis uses data from PbPb collisions at a centre-of-mass energy of 2.76 TeV per nucleon pair corresponding to an integrated luminosity of $150 \mu\text{b}^{-1}$ recorded by the CMS experiment at the LHC. For events containing an isolated photon with transverse momentum $p_T^\gamma > 60 \text{ GeV}/c$ and an associated jet with $p_T^{\text{jet}} > 30 \text{ GeV}/c$, the photon+jet p_T imbalance is studied as a function of collision centrality and compared to pp data and PYTHIA calculations at the same collision energy. Using the p_T^γ of the isolated photon as an estimate of the momentum of the associated parton at production, this measurement allows a characterisation of the in-medium parton energy loss. For more central PbPb collisions, a significant decrease in the ratio $p_T^{\text{jet}}/p_T^\gamma$ relative to that in the PYTHIA reference is observed. Furthermore, significantly more $p_T^\gamma > 60 \text{ GeV}/c$ photons in PbPb are observed not to have an associated $p_T^{\text{jet}} > 30 \text{ GeV}/c$ jet, compared to the reference. However, no significant broadening of the photon+jet azimuthal correlation is observed.

Submitted to Physics Letters B

*See Appendix A for the list of collaboration members

1 Introduction

Parton scatterings with large momentum transfer produce energetic particles which can be used as “probes” to study the strongly interacting medium created in high-energy heavy ion collisions [1, 2]. The production of high transverse momentum (p_T) partons and photons in “hard” processes occurs over very short time scales, $\tau \approx 1/p_T \lesssim 0.1 \text{ fm}/c$, and thus their yields can be potentially modified by final-state interactions occurring while they traverse the medium. Since the production cross sections of these energetic particles are calculable using perturbative quantum chromodynamics, they have long been recognised as particularly useful “tomographic” probes of the created medium [3–9].

In PbPb collisions at the Large Hadron Collider (LHC), the effects of the produced medium have been studied using back-to-back dijets which were observed to be significantly unbalanced in their transverse momenta [10–12]. The advantage of the large yield of dijets (as compared to photon+jet pairs) is, however, offset by a loss of information about the initial properties of the probes, i.e. prior to their interactions with the medium. Correlating two probes that both undergo energy loss also induces a selection bias towards scatterings occurring at, and oriented tangential to, the surface of the medium. At leading order (LO), photons are produced back-to-back with an associated parton (jet) having close to the same transverse momentum. Furthermore, these photons do not strongly interact with the medium. The yields of isolated photons in PbPb collisions were found to match the expectation based on pp data and the number of nucleon-nucleon collisions, with a modification factor of $R_{AA} = 0.99 \pm 0.31(\text{stat.}) \pm 0.26(\text{sys.})$ [13]. Therefore, photon+jet production has been hailed as the “golden channel” to investigate energy loss of partons in the medium [14, 15].

“Prompt photons” are photons produced directly in the hard sub-processes. Experimentally, events with enriched production of prompt photons are selected using an isolation requirement, namely that the additional energy in a cone of fixed radius around the direction of the reconstructed photon be less than a specified value [13]. This restriction yields “isolated photons” (γ), which consist mostly of prompt photons produced directly in the initial hard scattering. Background photons from the decays of neutral mesons, such as π^0 , η , and ω , are suppressed by this isolation requirement, as they are predominantly produced via jet fragmentation.

This Letter describes the first study of the jet energy loss using isolated-photon+jet pairs from PbPb data at a nucleon-nucleon centre-of-mass energy $\sqrt{s_{NN}} = 2.76 \text{ TeV}$. An integrated PbPb luminosity of $\int \mathcal{L} dt = 150 \mu\text{b}^{-1}$ was collected by the Compact Muon Solenoid (CMS) experiment during the 2011 running of the LHC. For comparison, a pp reference dataset with $\int \mathcal{L} dt \approx 200 \text{ nb}^{-1}$ at $\sqrt{s} = 2.76 \text{ TeV}$ was obtained in 2011.

The goal of this analysis is to characterise possible modifications of jet properties as a function of centrality using isolated-photon+jet events in PbPb collisions. The properties of isolated-photon+jet pairs are studied via the azimuthal angular correlation in $\Delta\phi_{J\gamma} = |\phi^{\text{jet}} - \phi^\gamma|$ and the transverse momentum ratio given by $x_{J\gamma} = p_T^{\text{jet}}/p_T^\gamma$. Photons with transverse momentum of $p_T^\gamma > 60 \text{ GeV}/c$ are selected in a pseudorapidity range of $|\eta^\gamma| < 1.44$, using isolation criteria detailed in Sections 2.2 and 2.3. These photons are then correlated with jets having $p_T^{\text{jet}} > 30 \text{ GeV}/c$ and $|\eta^{\text{jet}}| < 1.6$. Parton energy loss due to induced gluon radiation can lead to a shift of the $x_{J\gamma}$ distribution towards lower values. In addition, parton energy loss can cause reconstructed jets to fall below the $p_T^{\text{jet}} > 30 \text{ GeV}/c$ threshold, leading to a reduction of the fraction of photons with an associated jet.

Section 2 of this Letter begins with a description of the experimental setup as well as the event

triggering, selection and characterisation. The Monte Carlo simulation, the photon and jet reconstruction, and the analysis procedure are also described. The results and their systematic uncertainties are presented in Section 3, followed by a summary in Section 4.

2 The CMS detector

Particles produced in pp and PbPb collisions are studied using the CMS detector [16]. The central tracking system is comprised of silicon pixel and strip detectors that allow for the reconstruction of charged-particle trajectories in the pseudorapidity range $|\eta| < 2.5$, where $\eta = -\ln[\tan(\theta/2)]$ and θ is the polar angle relative to the counterclockwise beam direction. Photons are reconstructed using the energy deposited in the barrel region of the PbWO₄ crystal electromagnetic calorimeter (ECAL), which covers a pseudorapidity range of $|\eta| < 1.479$, and has a finely segmented granularity of $\Delta\eta \times \Delta\phi = 0.0174 \times 0.0174$. The brass/scintillator hadron calorimeter (HCAL) barrel region covers $|\eta| < 1.74$, and has a segmentation of $\Delta\eta \times \Delta\phi = 0.087 \times 0.087$. Endcap regions of the HCAL and ECAL extend the $|\eta|$ coverage out to about 3. The calorimeters and tracking systems are located within the 3.8 T magnetic field of the superconducting solenoid. In addition to the barrel and endcap detectors, CMS includes hadron forward (HF) steel/quartz-fibre Cherenkov calorimeters, which cover the forward rapidity of $2.9 < |\eta| < 5.2$ and are used to determine the degree of overlap (“centrality”) of the two colliding Pb nuclei [17]. A set of scintillator tiles, the beam scintillator counters, is mounted on the inner side of each HF for triggering and beam-halo rejection for both pp and PbPb collisions.

2.1 Trigger and event selection

Collision events containing high- p_T photon candidates are selected online by the CMS two-level trigger system consisting of the Level-1 (L1) and High Level Trigger (HLT). First, events are selected using an inclusive single-photon-candidate L1 trigger with a transverse momentum threshold of 5 GeV/ c . Then, more refined photon candidates are reconstructed in the HLT using a clustering algorithm (identical to that used for offline analysis) applied to energy deposits in the ECAL. Events containing a reconstructed photon candidate with $p_T^\gamma > 40$ GeV/ c are stored for further analysis. This HLT selection is fully efficient for events containing a photon with $p_T^\gamma > 50$ GeV/ c and the analysis presented here includes all photons with $p_T^\gamma > 60$ GeV/ c .

In order to select a pure sample of inelastic hadronic PbPb collisions for analysis, further offline selections were applied to the triggered event sample similar to [11]. Notably among these include requiring a reconstructed event vertex, and requiring at least 3 calorimeter towers in the HF on both sides of the interaction point with at least 3 GeV total deposited energy in each tower. Beam halo events were vetoed based on the timing of the $+z$ and $-z$ BSC signals. Additionally, events containing HCAL noise [18] are rejected to remove possible contamination of the jet sample. Details about this event selection scheme can be found in [10]. The number of events removed by these criteria are shown in Table 1. Analysis of the Monte Carlo (MC) reference, described in Section 2.2, uses identical event selection, except for the calorimeter noise rejection, which is a purely experimental effect.

The online trigger scheme for the pp data at 2.76 TeV is the same as that used for the CMS pp prompt photon analysis at 7 TeV [19]. The pp trigger requires at least one reconstructed electromagnetic cluster with a minimum transverse energy of 15 GeV/ c . The offline criterion applied to select pp hadronic collision events is similar to previous CMS pp papers [20]. Apart from the trigger and hadronic collision selection the pp analysis uses the same event selections as the PbPb analysis [13].

Table 1: The impact of the various event-selection criteria on the $\int \mathcal{L} dt = 150 \text{ mb}^{-1}$ PbPb data sample. In the third column, the percentages are with respect to the line above. The selections are applied in the sequence listed. Recall that $\Delta\phi_{J\gamma} = |\phi^{\text{Jet}} - \phi^\gamma|$.

Selection	Events remaining	% of previous
Collision events with a photon of $p_T^\gamma > 40 \text{ GeV}/c$	252576	–
HCAL cleaning	252317	96.76
Isolated photon candidate $p_T^\gamma > 60 \text{ GeV}/c, \eta < 1.44$	2974	1.18
Jet candidate $p_T^{\text{Jet}} > 30 \text{ GeV}/c, \eta < 1.6$	2198	73.91
$\Delta\phi_{J\gamma} > \frac{7}{8}\pi$	1535	69.84

For the analysis of PbPb events, it is important to determine the degree of overlap between the two colliding nuclei, termed collision centrality. Centrality is determined using the sum of transverse energy reconstructed in the HF. The distribution of this total energy is used to divide the event sample into equal percentiles of the total nucleus-nucleus interaction cross section. These finer centrality bins are then combined into four groups; one containing the 10% most central events (i.e. those which have the smallest impact parameter of the two colliding Pb nuclei and which produce the highest HF energy); two encompassing the next most central 10–30% and 30–50% of the events; and finally one with the remaining 50–100% peripheral events. Centrality can also be characterised using the number of nucleons participating in the interaction, N_{part} (with $N_{\text{part}} = 2$ for pp). The corresponding N_{part} values for a given centrality range are determined from a Glauber calculation [21]. Detector effects are accounted for using a GEANT4 simulation [22] of events generated with a multi-phase transport model (AMPT) [23]. A detailed description of the centrality determination procedure can be found in [10].

2.2 Monte Carlo simulation

The production of high- p_T photons by LO processes and parton radiation and fragmentation channels with a high- p_T photon in the final state are simulated with PYTHIA [24] (version 6.422, tune Z2). Tune Z2 is identical to the Z1 tune described in [25], except that Z2 uses the CTEQ6L PDF while Z1 uses CTEQ5L, and the cut-off for multiple parton interactions, $p_{\perp 0}$, at the nominal energy of $\sqrt{s_0} = 1.8 \text{ TeV}$ is decreased by $0.1 \text{ GeV}/c$. Modifications to account for the isospin effect of the colliding nuclei, i.e. the correct cross section weighting of pp, pn, and nn subcollisions [26], is used. Events containing isolated photons are selected using the generator-level information of the PYTHIA events. The isolation criterion requires that the total energy within a cone of radius $\Delta R = \sqrt{(\Delta\eta)^2 + (\Delta\phi)^2} = 0.4$ surrounding the photon direction be less than 5 GeV . This selection is found to be equivalent to the experimental requirements for isolated photons described in Section 2.3. These events are then processed through the full CMS detector simulation chain using the GEANT4 package. In order to model the effect of the underlying PbPb events, the PYTHIA photon events are embedded into background events generated using HYDJET (v 1.8) [26]. This version of HYDJET is tuned to reproduce event properties such as charged hadron multiplicity, p_T spectra, and elliptic flow measured as a function of centrality in PbPb collisions.

2.3 Photon reconstruction and identification

Photon candidates are reconstructed from clusters of energy deposited in the ECAL, following the method detailed in Ref. [13]. The selected photon candidates are restricted to be in the barrel region of the ECAL by requiring a pseudorapidity limit of $|\eta^\gamma| < 1.44$ and are also

required to have a transverse momentum of $p_T^\gamma > 60 \text{ GeV}/c$. In addition, photon candidates are dropped if they overlap with any electron tracks. Electrons are identified by matching tracks with reconstructed ECAL clusters and putting a cut on the ratio of calorimeter energy over track momentum. The separation of the photon and electron is required to be within a search window of $|\eta^\gamma - \eta^{\text{Track}}| < 0.02$ and $|\phi^\gamma - \phi^{\text{Track}}| < 0.15$. Anomalous signals caused by the interaction of heavily-ionising particles directly with the silicon avalanche photodiodes used for the ECAL barrel readout are removed, again using the prescription of Ref. [13]. The reconstructed photon energy is corrected to account for the material in front of the ECAL and for electromagnetic shower containment. An additional correction is applied to the clustered energy in order to remove the effects from the PbPb underlying event (UE). The size of the combined correction is obtained from the isolated photon PYTHIA + HYDJET sample and varies from 2–10%, depending on centrality and photon p_T^γ . The effect of the corrections on the energy scale is validated by an analysis of the reconstructed Z boson mass observed in $Z \rightarrow e^-e^+$ decays in PbPb data as a function of centrality.

Since the dominant source of neutral mesons is jet fragmentation with associated hadrons, a first rejection of neutral mesons mimicking a high- p_T photon in the ECAL is done using the ratio of hadronic to electromagnetic energy, H/E . The H/E ratio is calculated using the energy depositions in the HCAL and the ECAL inside a cone of $\Delta R = 0.15$ around the photon candidate direction [19]. Photon candidates with $H/E < 0.1$ are selected for this analysis. A correction for the contribution from the remaining short-lived neutral mesons is applied later.

To determine if a photon candidate is isolated, the detector activity in a cone of radius $\Delta R = 0.4$ with respect to the centroid of the cluster is used. The UE-subtracted photon isolation variable $\text{SumIso}^{\text{UE-sub}}$, which is the sum of transverse energy measured in three sub-detectors (ECAL, HCAL, Tracker) minus the expected contribution from the UE to each sub-detector, as described in [13], is used to further reject photon candidates originating from jets. The mean of $\text{SumIso}^{\text{UE-sub}}$ for fragmentation and decay photons is $\approx 20 \text{ GeV}$, while the distributions of $\text{SumIso}^{\text{UE-sub}}$ for isolated photons are Gaussians centred around 0 and having widths varying from 3.5 GeV for peripheral collisions to 8.5 GeV for central collisions. Candidates with $\text{SumIso}^{\text{UE-sub}}$ smaller than 1 GeV are selected for further study. A tightened isolation criterion for data (as compared to the 5 GeV applied for the MC) is used in order to minimise the impact of random PbPb UE fluctuations. A downward fluctuation in the UE contribution to $\text{SumIso}^{\text{UE-sub}}$ can inadvertently allow a non-isolated photon candidate to pass the isolation cut. From the PYTHIA + HYDJET sample, the fraction of photons surviving this tightened selection is estimated to be 70–85%, depending on centrality and photon p_T , and is found not to be dependent on the angular or momentum correlation with the associated jet. The relative efficiency of $\text{SumIso}^{\text{UE-sub}} < 1 \text{ GeV}$ compared to $\text{SumIso}^{\text{UE-sub}} < 5 \text{ GeV}$ ranges from 82% (0–10% centrality) to 90% (50–100% centrality). At the same time, the photon purity, central to peripheral, is 74–83% for the $\text{SumIso}^{\text{UE-sub}} < 1 \text{ GeV}$ cut, compared to 52–62% for the $\text{SumIso}^{\text{UE-sub}} < 5 \text{ GeV}$ cut.

Photon purities in each centrality interval are estimated using a two-component fit of the shape of the electromagnetic shower in the ECAL, $\sigma_{\eta\eta}$, defined as a modified second moment of the electromagnetic energy cluster distribution around its mean η position:

$$\sigma_{\eta\eta}^2 = \frac{\sum_i w_i (\eta_i - \bar{\eta})^2}{\sum_i w_i}, \quad (1)$$

$$w_i = \max\left(0, 4.7 + \ln \frac{E_i}{E}\right),$$

where E_i and η_i are the energy and position of the i -th ECAL crystal in a group of 5×5 crystals

centred on the one with the highest energy, E is the total energy of the crystals in the calculation, and $\bar{\eta}$ is the average η weighted by w_i in the same group [19]. The discrimination is based only on the pseudorapidity (i.e. longitudinal) distribution of the shower, which is aligned with the magnetic field direction. As a result, showers with a wider distribution in the transverse plane, which can originate from photons converted to e^+e^- pairs in the detector material, are not eliminated. The shape of the $\sigma_{\eta\eta}$ distribution for the signal is obtained from photon+jet PYTHIA + HYDJET samples for each p_T^γ and centrality bin. The shape of the background distribution is extracted from data using a background-enriched set of photon candidates with $10 < \text{SumIso}^{\text{UE-sub}} < 20$ GeV. The estimated photon purity (one minus the nonphoton contamination) is 74–83% for photon candidates, which are required to have $\sigma_{\eta\eta} < 0.01$.

2.4 Jet reconstruction

Jets are reconstructed by clustering particles measured with a particle-flow (PF) algorithm [27], using the anti- k_T sequential recombination algorithm with a distance parameter of $R = 0.3$ [28]. The jets used in the analysis are required to have $p_T^{\text{Jet}} > 30$ GeV/ c and $|\eta^{\text{Jet}}| < 1.6$ to ensure high reconstruction efficiency. Jets within $R < 0.3$ around a photon are removed in order not to correlate the photon with itself. Details of the jet reconstruction procedure and its performance can be found in [12]. The small value of R , compared to a more typical $R = 0.5$ – 0.7 used to analyse pp events, helps to minimise sensitivity to the UE contribution, and especially its fluctuations. The energy from the UE is subtracted using the same method as employed in [10, 12] and originally described in [29]. The jet energy resolution can be quantified using the Gaussian standard deviation σ of $p_T^{\text{Reco}}/p_T^{\text{Gen}}$, where p_T^{Reco} is the UE-subtracted, detector-level jet energy, and p_T^{Gen} is the generator-level jet energy without any contributions from a PbPb UE. The magnitude of this resolution is determined using PYTHIA + HYDJET simulation propagated through the detector using GEANT4. Compared to direct embedding into PbPb events, this method avoids uncertainties associated with the detector versus MC geometry alignment, which is especially difficult to achieve accurately with finely segmented pixel trackers. The UE produced by HYDJET with GEANT4 has been checked against the data by observing the energy collected inside randomly oriented cones with the same radius as the distance parameter in the jet algorithm. Data and MC are found to be well matched. The dependence of the jet resolution, σ , defined as the standard deviation of the reconstructed over the event generator p_T^{Jet} , can be parametrised using the expression

$$\sigma \left(\frac{p_T^{\text{Reco}}}{p_T^{\text{Gen}}} \right) = C \oplus \frac{S}{\sqrt{p_T^{\text{Gen}}}} \oplus \frac{N}{p_T^{\text{Gen}}}, \quad (2)$$

where \oplus indicates a sum in quadrature, and the quantities C , S , and N are fitted parameters (Table 2). The first two terms of the parametrisation are determined from PYTHIA simulation, and the third term, which represents background fluctuations (not corrected for the flow direction), is determined from PYTHIA + HYDJET simulation.

Because the effects of the UE for jets found in PbPb events are subtracted, corrections to the mean reconstructed jet energy are derived from pp data and PYTHIA-only simulation (i.e. without HYDJET) [30]. Studies of the performance of jet reconstruction in PYTHIA + HYDJET events show that no additional centrality-dependent energy correction is needed.

The jet reconstruction efficiency is defined as the fraction of simulated PYTHIA jets which are correctly reconstructed when embedded into a HYDJET event. The efficiency is found to be greater than 90% for jets within the selected p_T and η range for all centralities. For the analysis of the pp sample, the same PbPb jet reconstruction algorithm is used. The performance of the jet reconstruction in peripheral PbPb events is found to approach that for the pp simulation.

Table 2: Parameters of the functional form for the jet energy resolution $\sigma (p_T^{\text{Reco}} / p_T^{\text{Gen}})$ given in Eq. (2), obtained from GEANT4 simulation of PYTHIA pp jets and from PYTHIA jets embedded in HYDJET events for various PbPb centralities (indicated by the % ranges in parentheses). The units of S are $\sqrt{\text{GeV}/c}$ and the units of N are GeV/c .

C	S	N (pp)	N (50–100%)	N (30–50%)	N (10–30%)	N (0–10%)
0.0246	1.213	0.001	0.001	3.88	5.10	5.23

2.5 Analysis procedure

To construct photon+jet pairs, the highest p_T^γ isolated photon candidate in each selected event is associated with every jet in the same event. The photon+jet pairs constructed in this way contain background contributions that need to be subtracted before using them to study energy loss effects on the jet produced in the same scattering as the photon. The dominant background contributions are photons from meson decays which pass the isolation requirement and the combinatoric background where the leading photon is paired with a jet not originating from the same hard scattering. The combinatoric background includes misidentified jets which arise from fluctuations of the underlying event as well as real jets from multiple hard interactions in the collision.

The background contributions from decay photon and fake jets are estimated separately with methods that are data-driven and are subtracted from the photon+jet pair sample.

The estimation of the yield and the kinematic characteristics of decay photons contained in the isolated-photon sample is based on the shower shape distributions for the analysed ECAL clusters. The ECAL clusters originating from high- p_T meson decays correspond to two photons that are reconstructed as a single wide cluster. Events with a large shower width ($0.011 < \sigma_{\eta\eta} < 0.017$, see Eq. (1)) are used to determine the contributions of the decay photon background to the $\Delta\phi_{J\gamma}$ and $x_{J\gamma}$ observables. The background shape obtained from this procedure is scaled according to the background-photon fraction, which is estimated from a fit of the shower shape distribution. The estimated background contribution fraction (which is equal to $1 - \text{purity}$) is then subtracted from the yield for the signal events, which have a small shower width ($\sigma_{\eta\eta} < 0.01$).

The background contribution due to photon+jet pairs arising from fake jets or multiple hard scatterings is also subtracted. It is estimated by correlating each isolated highest- p_T photon from the triggered photon+jet sample to jets found in a different event selected randomly from a set of minimum bias PbPb data. The random event used in the pairing is chosen to have the same centrality as the photon+jet candidate event. The fake jet background estimated in this way has a flat distribution in $\Delta\phi_{J\gamma}$. The effect of this background is biggest in the most central events where, on average, approximately 20% of the jets paired with each photon candidate are estimated to be fake jets. The estimated distributions of $\Delta\phi_{J\gamma}$ and $x_{J\gamma}$ for photons paired with fake jets, found using this random pairing of events, are subtracted from the distributions coming from the same-event photon+jet sample to obtain the final results.

To determine the sensitivity to a potentially modified jet fragmentation, which may cause the reconstructed jet energy scale to deviate from the PYTHIA derived calibration, the MC studies were repeated but now using PYQUEN [26] jets embedded into HYDJET. PYQUEN simulates parton energy loss by radiative and collisional mechanisms, where a portion of the original parton energy is redistributed into gluons that are found largely outside the cone of the surviving jet. The PYQUEN+HYDJET events were run through the full detector simulation and then recon-

structured with the standard analysis. The jet modification in PYQUEN produces a photon+jet momentum imbalance comparable to that observed in our measurement (although in detail, with different $x_{J\gamma}$ distribution and N_{part} dependence). The extracted momentum imbalance was found to reproduce the generator level imbalance well within the statistical uncertainties. We also note that a similar insensitivity to differences among QCD fragmentation was found previously by studying the jet energy scale from separate PYTHIA gluon and light quark jets, which differ significantly in their fragmentation patterns [31]. The standard analysis using PF jets was cross checked using jets reconstructed with only information from the calorimeters. This alternative analysis has different corrections for jet energy scale and resolution and a different sensitivity to low momentum tracks. The two analyses give comparable results for the photon+jet observables.

3 Results

3.1 Photon+jet azimuthal correlations

Possible medium effects on the back-to-back alignment of the photon and recoiling jet can be studied using the distribution of the number of photon+jet pairs, $N_{J\gamma}$, as a function of the relative azimuthal angle, $\Delta\phi_{J\gamma}$, normalised the total number of pairs, $(N_{J\gamma})^{-1}dN_{J\gamma}/d\Delta\phi_{J\gamma}$. Figure 1 shows distributions of $\Delta\phi_{J\gamma}$ for PbPb data in four centrality bins, ranging from peripheral events (50–100%, Fig. 1a) to the most central events (0–10%, Fig. 1d). The PbPb data are compared to PYTHIA + HYDJET simulation and pp data. For both PbPb data and MC distributions, the jet is found to be well aligned opposite to the photon direction, with a clear peak at $\Delta\phi_{J\gamma} = \pi$. The shape of the $\Delta\phi_{J\gamma}$ correlation peak is similar in PbPb data and MC. The apparent excess in the tail of the 0–10% data was investigated and deemed statistically not significant compared to the subtracted background. To study the centrality evolution of the shape, the distributions are fitted to a normalised exponential function:

$$\frac{1}{N_{J\gamma}} \frac{dN_{J\gamma}}{d\Delta\phi_{J\gamma}} = \frac{e^{(\Delta\phi - \pi)/\sigma}}{(1 - e^{-\pi/\sigma})\sigma}. \quad (3)$$

The fit is restricted to the exponentially falling region $\Delta\phi > 2\pi/3$. The results of this fit for PbPb data are shown in Fig. 2, where the width of the azimuthal correlation (σ in Eq. (3), denoted $\sigma(\Delta\phi_{J\gamma})$ in Fig. 2) is plotted as a function of centrality and compared to pp and PYTHIA + HYDJET fit results. The resulting $\sigma(\Delta\phi_{J\gamma})$ values in PbPb do not show a significant centrality dependence within the present statistical and systematic uncertainties. For central PbPb collisions, $\sigma(\Delta\phi_{J\gamma})$ is similar to the PYTHIA reference based on the Z2 tune, and comparison with other PYTHIA tunes shows a theoretical uncertainty that is larger than the difference between the data and MC. Comparing the PYTHIA tune Z2 with tune D6T [32, 33] shows an 8% difference in $\sigma(\Delta\phi_{J\gamma})$, which is expected because these two tunes differ in their parton shower ordering resulting in a different $\Delta\phi$ correlation. The large statistical uncertainty in the $\sigma(\Delta\phi_{J\gamma})$ extracted from the pp data at 2.76 TeV does not allow a discrimination between these two PYTHIA tunes. Both the Z2 and D6T tunes matched the shape of the azimuthal dijet correlation measured in pp collisions at 7 TeV [34] at about the 10% level in the region $\Delta\phi > 2\pi/3$. The result that $\sigma(\Delta\phi_{J\gamma})$ is not found to be significantly modified by the medium is consistent with the earlier observation of an unmodified $\Delta\phi$ correlation in dijet events [10].

3.2 Photon+jet momentum imbalance

The asymmetry ratio $x_{J\gamma} = p_T^{\text{jet}}/p_T^\gamma$ is used to quantify the photon+jet momentum imbalance. In addition to the jet and photon selections used in the $\Delta\phi_{J\gamma}$ study, we further impose a strict

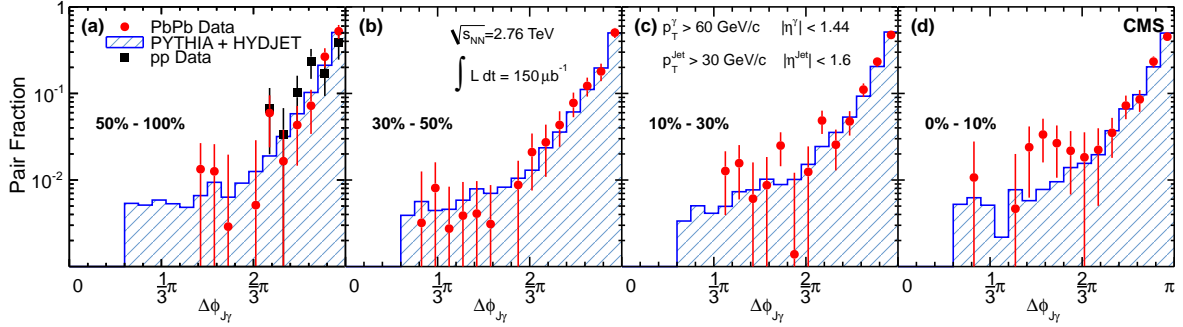


Figure 1: Azimuthal correlation $\Delta\phi_{J\gamma}$ between the photon and associated jet after background subtraction. The area of each distribution is normalised to unity. All panels show PbPb data (filled circles) compared to pp data at 2.76 TeV (filled squares), and to the PYTHIA + HYDJET MC simulation (shaded histogram) in bins of increasing centrality left to right. The error bars on the points represent the statistical uncertainty.

$\Delta\phi_{J\gamma} > \frac{7}{8}\pi$ cut to suppress contributions from background jets. Note that photon+jet pairs for which the associated jet falls below the 30 GeV/c threshold are not included in the $x_{J\gamma}$ calculation. This limits the bulk of the $x_{J\gamma}$ distribution to $x_{J\gamma} \gtrsim 0.5$. Figure 3 shows the centrality dependence of $x_{J\gamma}$ for PbPb collisions as well as that for PYTHIA + HYDJET simulation where PYTHIA contains inclusive isolated photon processes. The $\langle x_{J\gamma} \rangle$ obtained from PYTHIA tunes Z2 and D6T agree to better than 1%. Overlaid in the peripheral bin is the $\langle x_{J\gamma} \rangle$ for 2.76 TeV pp data, showing consistency to the MC reference. However the poor statistics of the pp data and the 50–100% PbPb centrality bin do not offer a strong constraint on a specific MC reference. However, further studies using the 7 TeV high statistics pp data showed a good agreement in $\langle x_{J\gamma} \rangle$ between data and PYTHIA, justifying the use of PYTHIA + HYDJET as an un-modified reference. The dominant source of systematic uncertainty in $\langle x_{J\gamma} \rangle$ is the relative photon+jet energy scale. Its impact on the probability density of $x_{J\gamma}$ is approximately 10% for the intermediate region of $0.6 < x_{J\gamma} < 1.2$. The normalisation to unity causes a point-to-point anticorrelation in the systematic uncertainties, where the upward movement of the probability density at small $x_{J\gamma}$ has to be offset by the corresponding downward movement at large $x_{J\gamma}$. This is represented by the separate open and shaded red systematic uncertainty boxes in Fig. 3. For a given change in the energy scale, all points would move together in the direction of either the open or shaded red box. The N_{part} dependence of the mean value $\langle x_{J\gamma} \rangle$ is shown in Fig. 4(a).

While the photon+jet momentum ratio in the PYTHIA + HYDJET simulation shows almost no change in the peak location and only a modest broadening, even in the most central PbPb events, the PbPb collision data exhibit a change in shape, shifting the distribution towards lower $x_{J\gamma}$ as a function of centrality. It is important to note that, as discussed above, the limitation of $x_{J\gamma} \gtrsim 0.5$ limits the degree to which this distribution can shift.

3.3 Jet energy loss

To study the quantitative centrality evolution of the energy loss, the average ratio of the jet and photon transverse momenta, $\langle x_{J\gamma} \rangle$, is shown in Fig. 4(a). While the photon+jet mean momentum ratio in the PYTHIA + HYDJET simulation exhibits a roughly centrality-independent value of $\langle x_{J\gamma} \rangle = 0.847 \pm 0.004(\text{stat.}) - 0.859 \pm 0.005(\text{stat.})$, the ratio is $\langle x_{J\gamma} \rangle = 0.73 \pm 0.02(\text{stat.}) \pm 0.04(\text{syst.})$ in the most central PbPb data, indicating that the presence of the medium results in more unbalanced photon+jet pairs.

It is important to keep in mind that the average energy loss of the selected photon+jet pairs does

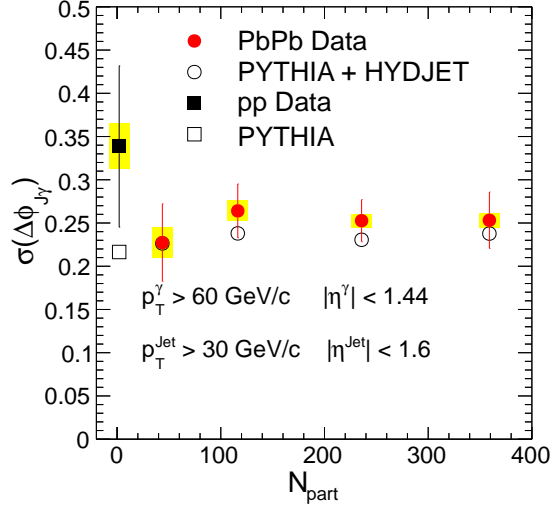


Figure 2: Fitted $\Delta\phi_{J\gamma}$ width (σ in Eq. (3)) between the photon and associated jet after background subtraction as a function of N_{part} . The fit range was restricted to $\Delta\phi_{J\gamma} > \frac{2}{3}\pi$. The yellow boxes indicate point-to-point systematic uncertainties and the error bars denote the statistical uncertainty.

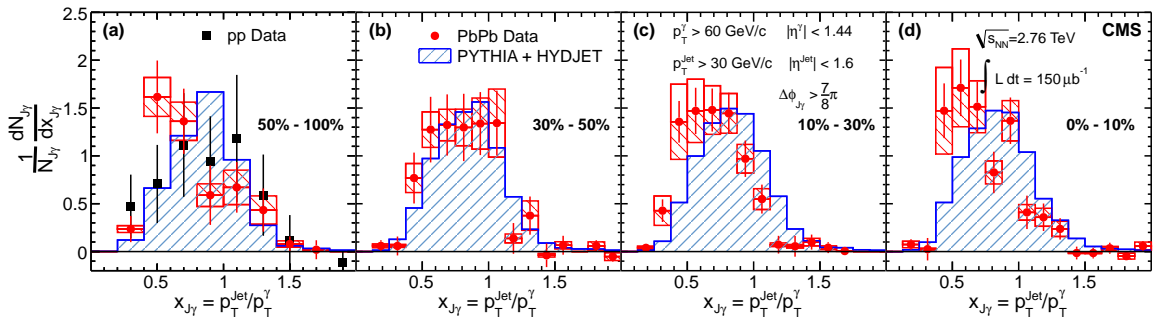


Figure 3: Ratio of p_T between the photon ($p_T^\gamma > 60 \text{ GeV}/c$) and jet ($p_T^{\text{jet}} > 30 \text{ GeV}/c$, $\Delta\phi_{J\gamma} > \frac{7}{8}\pi$) after subtracting background. The area of each distribution is normalised to unity. All panels show PbPb data (filled circles) compared to pp data at 2.76 TeV (filled squares), and to the PYTHIA + HYDJET MC simulation (shaded histogram) in bins of increasing centrality left to right. The error bars on the points represent the statistical uncertainty. See text for an explanation of the open and shaded red systematic uncertainty boxes.

not constitute the full picture. There are genuine photon+jet events which do not contribute to the $\langle x_{J\gamma} \rangle$ distribution because the associated jet falls below the $p_T^{\text{Jet}} > 30 \text{ GeV}/c$ threshold. To quantify this effect, Fig. 4(b) shows $R_{J\gamma}$, the fraction of isolated photons that have an associated jet passing the analysis selection. The value of $R_{J\gamma}$ is found to decrease, from $R_{J\gamma} = 0.685 \pm 0.008(\text{stat.}) - 0.698 \pm 0.006(\text{stat.})$ for the PYTHIA + HYDJET reference, as well as pp and peripheral PbPb data, to the significantly lower $R_{J\gamma} = 0.49 \pm 0.03(\text{stat.}) \pm 0.02(\text{syst.}) - 0.54 \pm 0.05(\text{stat.}) \pm 0.02(\text{syst.})$ for the three PbPb bins above 50% centrality.

An analysis with a lower p_T cutoff on the associated jet energy would result in values of $R_{J\gamma}$ closer to unity. This would shift the cutoff at low $x_{J\gamma}$ in Fig. 3 closer to zero. It is likely, although not certain, that these additional events would result in a larger deviation in $x_{J\gamma}$ between the PbPb data and the reference shown in Fig. 4(a).

3.4 Systematic uncertainties

Photon purity, reconstruction efficiency, and isolation, as well as the contamination from e^\pm and fake jets contribute to the systematic uncertainties of the photon+jet azimuthal correlation and the observables related to momentum asymmetry, $\langle x_{J\gamma} \rangle$ and $R_{J\gamma}$. Additionally, the momentum asymmetry observables are also influenced by the relative photon and jet energy calibrations. For the measurement of $\sigma(\Delta\phi)$, the uncertainty due to the photon angular resolution is negligible, less than 10^{-5} .

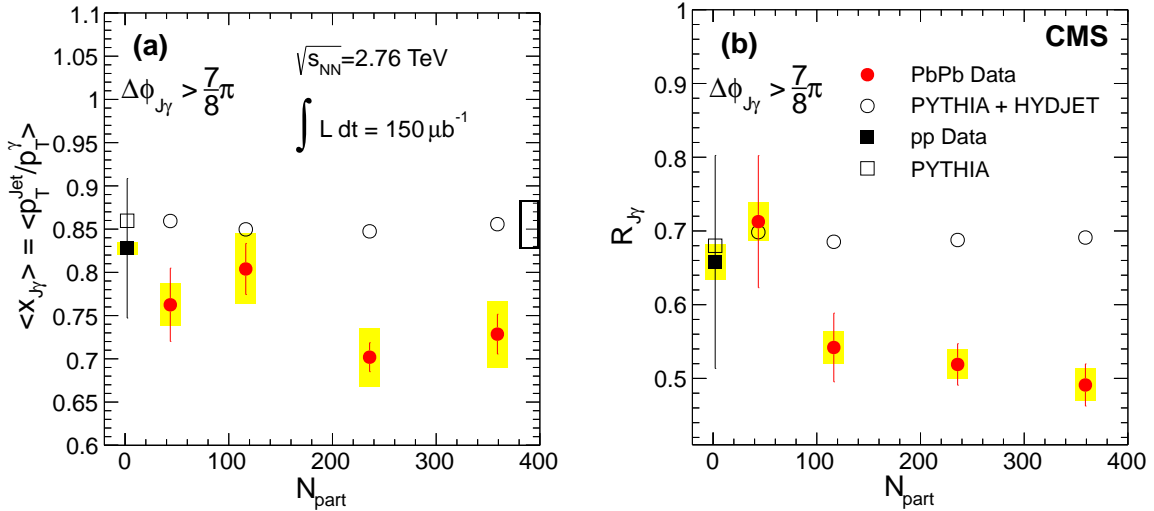


Figure 4: (a) Average ratio of jet transverse momentum to photon transverse momentum, $\langle x_{J\gamma} \rangle$, as a function of N_{part} . The empty box at the far right indicates the correlated systematic uncertainty. (b) Average fraction of isolated photons with an associated jet above 30 GeV/c, $R_{J\gamma}$, as a function of N_{part} . In both panels, the yellow boxes indicate point-to-point systematic uncertainties and the error bars denote the statistical uncertainty.

The uncertainty in the relative photon+jet energy scale consists of four main contributions. The first one comes from the 2% relative uncertainty of the jet energy scale in the barrel for $30 < p_T^{\text{Jet}} < 200 \text{ GeV}/c$, when compared with the ECAL energy scale [30]. The second contribution is the residual data-to-MC energy scale difference in pp collisions, which is not corrected for in this analysis, for which we quote the 2% maximum relative uncertainty which applies in the range $|\eta^{\text{jet}}| < 1.6$. Thirdly, the additional uncertainty for the jet energy scale in the presence of the UE is determined to be 3% for the 30 to 100% and 4% for the 0 to 30% centrality range,

using the embedding of PYTHIA isolated photon+jet pairs into HYDJET. The fourth contribution is the effect of heavy ion background on the ECAL energy scale, which is determined from $Z \rightarrow e^-e^+$ mass reconstruction, after applying the PbPb ECAL correction. This results in a relative uncertainty of 1.5%, comparable to the pp uncertainty (obtained via π^0 and $\eta \rightarrow \gamma\gamma$).

The absolute photon energy scale uncertainty, estimated to be 1.5% using Z decays as described above, will also affect the threshold of our photon kinematic selection. Similarly, the lower transverse momentum cutoff for jets is sensitive to their absolute energy scale. For CMS, the energy of jets is calibrated by measuring the relative photon+jet energy scale in pp collisions, and therefore the uncertainty in jet energies is the quadrature sum of the uncertainties in the relative jet-to-photon energy scale and the absolute photon energy scale.

The uncertainty of the photon purity measurement using the $\sigma_{\eta\eta}$ template fitting is estimated by (a) varying the selection of sideband regions that is used to obtain the background template and (b) shifting the template to measure the signal template uncertainty. These result in an estimated uncertainty on the photon purity of 12% and 2%, respectively. Systematic effects due to photon reconstruction efficiency are estimated by correcting the data using the efficiency derived from the MC simulation, and comparing the result with the uncorrected distribution. The contribution of non-isolated photons (mostly from jet fragmentation) that are incorrectly determined to be isolated in the detector due to UE energy fluctuations or detector resolution effects is estimated using PYTHIA + HYDJET simulation. The difference of photon+jet observables obtained from generator level isolated photons and detector level isolated photons is taken to be the systematic uncertainty resulting from the experimental criterion for an isolated photon.

The current analysis removes contamination from fake jets purely by subtracting the background estimated from event mixing. A cross-check of this subtraction has been performed using a direct rejection of fake jets via a fake jet discriminant. The discriminant sums the p_T^2 of the jet core within $R < 0.1$ around the jet axis and determines the likelihood that the reconstructed jet is not the result of a background fluctuation. Both techniques for fake jet removal agree within 1% for the observables studied. The effect of inefficiencies in the jet finding is estimated by repeating the analysis and weighting each jet with the inverse of the jet finding efficiency as a function of p_T^{Jet} .

Table 3: Relative systematic uncertainties for $\sigma(\Delta\phi_{J\gamma})$ for pp data and each of the PbPb centrality bins.

Source	pp	PbPb 50–100%	PbPb 30–50%	PbPb 10–30%	PbPb 0–10%
γ p_T threshold	3.0%	3.0%	3.0%	2.0%	1.2%
Jet p_T threshold	1.3%	1.3%	0.2%	0.5%	2.4%
γ efficiency	0.8%	0.8%	0.3%	0.3%	0.3%
Jet efficiency	0.6%	0.6%	0.7%	0.4%	0.3%
Isolated γ definition	0.7%	0.7%	1.6%	2.0%	0.5%
γ purity	6.8%	6.8%	2.7%	0.5%	0.9%
e^-, e^+ contamination	0.5%	0.5%	0.5%	0.5%	0.5%
Fake jet contamination	0.3%	0.3%	0.1%	0.2%	1.2%
Jet ϕ resolution	0.5%	0.5%	0.5%	0.5%	0.5%
σ fitting	0.3%	0.3%	0.1%	0.1%	0.1%
Total	7.7%	7.7%	4.5%	3.0%	3.2%

Tables 3, 4, and 5 summarise the relative systematic uncertainties for $\sigma(\Delta\phi)$, $\langle x_{J\gamma} \rangle$, and $R_{J\gamma}$,

Table 4: Relative systematic uncertainties for $\langle x_{J\gamma} \rangle$ for pp data and each of the PbPb centrality bins. The uncertainties due to the pp γ -jet relative energy scale and γ purity are common to all of the measurements and are quoted as a correlated uncertainty.

Source	pp	PbPb 50–100%	PbPb 30–50%	PbPb 10–30%	PbPb 0–10%
γ -jet rel. energy scale	2.8%	4.1%	5.4%	5.0%	4.9%
γ p_T threshold	0.6%	0.6%	0.6%	0.6%	1.3%
Jet p_T threshold	0.7%	0.7%	1.9%	1.9%	2.0%
γ efficiency	< 0.1%	< 0.1%	< 0.1%	0.1%	0.2%
Jet efficiency	0.5%	0.5%	0.6%	0.6%	0.5%
Isolated γ definition	0.1%	0.1%	0.7%	0.4%	2.0%
γ purity	2.2%	2.2%	1.9%	2.4%	2.7%
e^-, e^+ contamination	0.5%	0.5%	0.5%	0.5%	0.5%
Fake jet contamination	0.1%	0.1%	0.1%	0.2%	0.1%
Total	3.7%	4.8%	6.2%	6.0%	6.4%
Correlated (abs., rel.)	3.6%	3.6%	3.6%	3.6%	3.6%
Point-to-point	0.9%	3.2%	5.1%	4.8%	5.3%

Table 5: Relative systematic uncertainties for the fraction of photons matched with jets, $R_{J\gamma}$, for pp data and each of the PbPb centrality bins.

Source	pp	PbPb 50–100%	PbPb 30–50%	PbPb 10–30%	PbPb 0–10%
γ p_T threshold	2.0%	2.0%	1.9%	1.3%	2.1%
Jet p_T threshold	1.4%	1.4%	2.3%	2.6%	2.7%
γ efficiency	0.2%	0.2%	0.2%	0.5%	0.5%
Jet efficiency	1.5%	1.5%	1.7%	1.8%	2.1%
Isolated γ definition	0.2%	0.2%	0.6%	1.3%	0.8%
γ purity	2.3%	2.3%	1.9%	0.2%	0.9%
e^-, e^+ contamination	0.5%	0.5%	0.5%	0.5%	0.5%
Fake jet contamination	0.4%	0.4%	0.8%	1.0%	1.4%
Total	3.7%	3.7%	4.1%	3.9%	4.5%

respectively, for the pp data and for each of the PbPb centrality bins used in the analysis. For $\langle x_{J\gamma} \rangle$, the uncertainties are separated into a correlated component that is common to all centrality bins and a component that represents the point-to-point systematic uncertainty. The common correlated uncertainty is obtained by combining the pp jet energy scale uncertainty with the photon purity uncertainty. This absolute uncertainty of 3.6% was used as the correlated uncertainty for all PbPb centrality bins.

4 Conclusions

The first study of isolated-photon+jet correlations in PbPb collisions at $\sqrt{s_{NN}} = 2.76$ TeV has been performed as a function of collision centrality using a dataset corresponding to an integrated luminosity of $150 \mu\text{b}^{-1}$. Isolated photons with $p_T^\gamma > 60$ GeV/c were correlated with jets with $p_T^{\text{jet}} > 30$ GeV/c to determine the width of the angular correlation function, $\sigma(\Delta\phi_{J\gamma})$, the jet/photon transverse momentum ratio, $x_{J\gamma} = p_T^{\text{jet}}/p_T^\gamma$, and the fraction of photons with an associated jet, $R_{J\gamma}$. The PbPb data were compared to both pp data and a PYTHIA + HYDJET MC reference which included the effect of the underlying PbPb event but no parton energy loss. No angular broadening was observed beyond that seen in the pp data and MC reference at all centralities. The average transverse momentum ratio for the most central events was found to be $\langle x_{J\gamma} \rangle_{0-10\%} = 0.73 \pm 0.02(\text{stat.}) \pm 0.04(\text{syst.})$. This is lower than the value of 0.86 seen in the pp data and predicted by PYTHIA + HYDJET at the same centrality. In addition to the shift in momentum balance, it was found that, in central PbPb data, only a fraction equal to $R_{J\gamma} = 0.49 \pm 0.03(\text{stat.}) \pm 0.02(\text{syst.})$ of photons are matched with an associated jet at $\Delta\phi_{J\gamma} > \frac{7}{8}\pi$, compared to a value of 0.69 seen in PYTHIA + HYDJET simulation. Due to the hot and dense medium created in central PbPb collisions, the energy loss of the associated parton causes the corresponding reconstructed jet to fall below the $p_T^{\text{jet}} > 30$ GeV/c threshold for an additional 20% of the selected photons.

Acknowledgments

We congratulate our colleagues in the CERN accelerator departments for the excellent performance of the LHC machine. We thank the technical and administrative staff at CERN and other CMS institutes, and acknowledge support from: FMSR (Austria); FNRS and FWO (Belgium); CNPq, CAPES, FAPERJ, and FAPESP (Brazil); MES (Bulgaria); CERN; CAS, MoST, and NSFC (China); COLCIENCIAS (Colombia); MSES (Croatia); RPF (Cyprus); MoER, SF0690030s09 and ERDF (Estonia); Academy of Finland, MEC, and HIP (Finland); CEA and CNRS/IN2P3 (France); BMBF, DFG, and HGF (Germany); GSRT (Greece); OTKA and NKTH (Hungary); DAE and DST (India); IPM (Iran); SFI (Ireland); INFN (Italy); NRF and WCU (Korea); LAS (Lithuania); CINVESTAV, CONACYT, SEP, and UASLP-FAI (Mexico); MSI (New Zealand); PAEC (Pakistan); MSHE and NSC (Poland); FCT (Portugal); JINR (Armenia, Belarus, Georgia, Ukraine, Uzbekistan); MON, RosAtom, RAS and RFBR (Russia); MSTD (Serbia); MICINN and CPAN (Spain); Swiss Funding Agencies (Switzerland); NSC (Taipei); TUBITAK and TAEK (Turkey); STFC (United Kingdom); DOE and NSF (USA).

References

- [1] E. V. Shuryak, “Quark-gluon plasma and hadronic production of leptons, photons and pions”, *Phys. Lett. B* **78** (1978) 150, doi:10.1016/0370-2693(78)90370-2.

- [2] E. V. Shuryak, "What RHIC experiments and theory tell us about properties of quark-gluon plasma?", *Nucl. Phys. A* **750** (2005) 64, doi:10.1016/j.nuclphysa.2004.10.022, arXiv:hep-ph/0405066.
- [3] D. A. Appel, "Jets as a probe of quark-gluon plasmas", *Phys. Rev. D* **33** (1986) 717, doi:10.1103/PhysRevD.33.717.
- [4] J. P. Blaizot and L. D. McLerran, "Jets in expanding quark-gluon plasmas", *Phys. Rev. D* **34** (1986) 2739, doi:10.1103/PhysRevD.34.2739.
- [5] M. Gyulassy and M. Plumer, "Jet quenching in dense matter", *Phys. Lett. B* **243** (1990) 432, doi:10.1016/0370-2693(90)91409-5.
- [6] X.-N. Wang and M. Gyulassy, "Gluon Shadowing and Jet Quenching in A+A Collisions at $\sqrt{s} = 200A$ GeV", *Phys. Rev. Lett.* **68** (1992) 1480, doi:10.1103/PhysRevLett.68.1480.
- [7] R. Baier et al., "Radiative energy loss and p_{\perp} broadening of high-energy partons in nuclei", *Nucl. Phys. B* **484** (1997) 265, doi:10.1016/S0550-3213(96)00581-0, arXiv:hep-ph/9608322.
- [8] B. G. Zakharov, "Radiative energy loss of high-energy quarks in finite size nuclear matter and quark-gluon plasma", *JETP Lett.* **65** (1997) 615, doi:10.1134/1.567389, arXiv:hep-ph/9704255.
- [9] R. B. Neufeld, I. Vitev, and B.-W. Zhang, "Physics of Z^0/γ^* -tagged jets at energies available at the CERN Large Hadron Collider", *Phys. Rev. C* **83** (2011) 034902, doi:10.1103/PhysRevC.83.034902, arXiv:1006.2389.
- [10] CMS Collaboration, "Observation and studies of jet quenching in PbPb collisions at $\sqrt{s_{NN}} = 2.76$ TeV", *Phys. Rev. C* **84** (2011) 024906, doi:10.1103/PhysRevC.84.024906, arXiv:1102.1957.
- [11] ATLAS Collaboration, "Observation of a Centrality-Dependent Dijet Asymmetry in Lead-Lead Collisions at $\sqrt{s_{NN}} = 2.76$ TeV with the ATLAS Detector at the LHC", *Phys. Rev. Lett.* **105** (2010) 252303, doi:10.1103/PhysRevLett.105.252303, arXiv:1011.6182.
- [12] CMS Collaboration, "Jet momentum dependence of jet quenching in PbPb collisions at $\sqrt{s_{NN}} = 2.76$ TeV", (2012). arXiv:1202.5022. Submitted to *Phys. Lett. B*.
- [13] CMS Collaboration, "Measurement of isolated photon production in pp and PbPb collisions at $\sqrt{s_{NN}} = 2.76$ TeV", *Phys. Lett. B* **710** (2012) 256, doi:10.1016/j.physletb.2012.02.077.
- [14] X.-N. Wang, Z. Huang, and I. Sarcevic, "Jet Quenching in the Direction Opposite to a Tagged Photon in High-Energy Heavy-Ion Collisions", *Phys. Rev. Lett.* **77** (1996) 231, doi:10.1103/PhysRevLett.77.231, arXiv:9701227.
- [15] X.-N. Wang and Z. Huang, "Medium-induced parton energy loss in γ +jet events of high-energy heavy-ion collisions", *Phys. Rev. C* **55** (1997) 3047, doi:10.1103/PhysRevC.55.3047, arXiv:9605213.
- [16] CMS Collaboration, "The CMS experiment at the CERN LHC", *JINST* **03** (2008) S08004, doi:10.1088/1748-0221/3/08/S08004.

- [17] CMS Collaboration, “Dependence on pseudorapidity and centrality of charged hadron production in PbPb collisions at $\sqrt{s_{NN}} = 2.76$ TeV”, *JHEP* **08** (2011) 141, doi:10.1007/JHEP08(2011)141, arXiv:1107.4800.
- [18] CMS Collaboration, “Identification and filtering of uncharacteristic noise in the CMS hadron calorimeter”, *JINST* **05** (2010) T03014, doi:10.1088/1748-0221/5/03/T03014, arXiv:0911.4881.
- [19] CMS Collaboration, “Measurement of the Isolated Prompt Photon Production Cross Section in pp Collisions at $\sqrt{s} = 7$ TeV”, *Phys. Rev. Lett.* **106** (2011) 082001, doi:10.1103/PhysRevLett.106.082001, arXiv:1012.0799.
- [20] CMS Collaboration, “Charged particle transverse momentum spectra in pp collisions at $\sqrt{s} = 0.9$ and 7 TeV”, *JHEP* **08** (2011) 086, doi:10.1007/JHEP08(2011)086, arXiv:1104.3547.
- [21] M. L. Miller et al., “Glauber Modeling in High Energy Nuclear Collisions”, *Ann. Rev. Nucl. Part. Sci.* **57** (2007) 205, doi:10.1146/annurev.nucl.57.090506.123020, arXiv:nucl-ex/0701025.
- [22] GEANT4 Collaboration, “GEANT4—a simulation toolkit”, *Nucl. Instrum. Meth. A* **506** (2003) 250, doi:10.1016/S0168-9002(03)01368-8.
- [23] Z.-W. Lin et al., “A multiphase transport model for relativistic heavy ion collisions”, *Phys. Rev. C* **72** (2005) 064901, doi:10.1103/PhysRevC.72.064901, arXiv:nucl-th/0411110.
- [24] T. Sjöstrand, S. Mrenna, and P. Z. Skands, “PYTHIA 6.4 physics and manual”, *JHEP* **05** (2006) 026, doi:10.1088/1126-6708/2006/05/026, arXiv:hep-ph/0603175.
- [25] R. Field, “Early LHC Underlying Event Data — Findings and Surprises”, (2010). arXiv:1010.3558.
- [26] I. P. Lokhtin and A. M. Snigirev, “A model of jet quenching in ultrarelativistic heavy ion collisions and high- p_T hadron spectra at RHIC”, *Eur. Phys. J. C* **45** (2006) 211, doi:10.1140/epjc/s2005-02426-3, arXiv:hep-ph/0506189.
- [27] CMS Collaboration, “Commissioning of the Particle-Flow Reconstruction in Minimum-Bias and Jet Events from pp Collisions at 7 TeV”, CMS Physics Analysis Summary CMS-PAS-PFT-10-002, (2010).
- [28] M. Cacciari, G. P. Salam, and G. Soyez, “The anti- k_t jet clustering algorithm”, *JHEP* **04** (2008) 063, doi:10.1088/1126-6708/2008/04/063, arXiv:0802.1189.
- [29] O. Kodolova et al., “The performance of the jet identification and reconstruction in heavy ions collisions with CMS detector”, *Eur. Phys. J. C* **50** (2007) 117, doi:10.1140/epjc/s10052-007-0223-9.
- [30] CMS Collaboration, “Determination of jet energy calibration and transverse momentum resolution in CMS”, *JINST* **06** (2011) P11002, doi:10.1088/1748-0221/6/11/P11002, arXiv:1107.4277.
- [31] M. Nguyen et al., “Jet Reconstruction with Particle Flow in Heavy-Ion Collisions with CMS”, *J. Phys. G* **38** (2011) 124151, doi:10.1088/0954-3899/38/12/124151, arXiv:1107.0179.

-
- [32] R. Field, "Physics at the Tevatron", *Acta Phys. Polon. B* **39** (2008) 2611.
- [33] P. Bartalini and L. Fanò, "Multiple Parton Interactions Studies at CMS", (2011).
arXiv:1103.6201.
- [34] CMS Collaboration, "Dijet Azimuthal Decorrelations in pp Collisions at $\sqrt{s} = 7$ TeV",
Phys. Rev. Lett. **106** (2011) 122003, doi:10.1103/PhysRevLett.106.122003,
arXiv:1101.5029.

A The CMS Collaboration

Yerevan Physics Institute, Yerevan, Armenia

S. Chatrchyan, V. Khachatryan, A.M. Sirunyan, A. Tumasyan

Institut für Hochenergiephysik der OeAW, Wien, Austria

W. Adam, T. Bergauer, M. Dragicevic, J. Erö, C. Fabjan, M. Friedl, R. Frühwirth, V.M. Ghete, J. Hammer¹, N. Hörmann, J. Hrubec, M. Jeitler, W. Kiesenhofer, V. Knünz, M. Krammer, D. Liko, I. Mikulec, M. Pernicka[†], B. Rahbaran, C. Rohringer, H. Rohringer, R. Schöfbeck, J. Strauss, A. Taurok, P. Wagner, W. Waltenberger, G. Walzel, E. Widl, C.-E. Wulz

National Centre for Particle and High Energy Physics, Minsk, Belarus

V. Mossolov, N. Shumeiko, J. Suarez Gonzalez

Universiteit Antwerpen, Antwerpen, Belgium

S. Bansal, T. Cornelis, E.A. De Wolf, X. Janssen, S. Luyckx, T. Maes, L. Mucibello, S. Ochesanu, B. Roland, R. Rougny, M. Selvaggi, H. Van Haevermaet, P. Van Mechelen, N. Van Remortel, A. Van Spilbeeck

Vrije Universiteit Brussel, Brussel, Belgium

F. Blekman, S. Blyweert, J. D'Hondt, R. Gonzalez Suarez, A. Kalogeropoulos, M. Maes, A. Olbrechts, W. Van Doninck, P. Van Mulders, G.P. Van Onsem, I. Villella

Université Libre de Bruxelles, Bruxelles, Belgium

O. Charaf, B. Clerbaux, G. De Lentdecker, V. Dero, A.P.R. Gay, T. Hreus, A. Léonard, P.E. Marage, T. Reis, L. Thomas, C. Vander Velde, P. Vanlaer, J. Wang

Ghent University, Ghent, Belgium

V. Adler, K. Bernaert, A. Cimmino, S. Costantini, G. Garcia, M. Grunewald, B. Klein, J. Lellouch, A. Marinov, J. McCartin, A.A. Ocampo Rios, D. Ryckbosch, N. Strobbe, F. Thyssen, M. Tytgat, L. Vanelderen, P. Verwilligen, S. Walsh, E. Yazgan, N. Zaganidis

Université Catholique de Louvain, Louvain-la-Neuve, Belgium

S. Basegmez, G. Bruno, R. Castello, L. Ceard, C. Delaere, T. du Pree, D. Favart, L. Forthomme, A. Giammanco², J. Hollar, V. Lemaître, J. Liao, O. Militaru, C. Nuttens, D. Pagano, A. Pin, K. Piotrkowski, N. Schul, J.M. Vizán Garcia

Université de Mons, Mons, Belgium

N. Belyi, T. Caebergs, E. Daubie, G.H. Hammad

Centro Brasileiro de Pesquisas Físicas, Rio de Janeiro, Brazil

G.A. Alves, M. Correa Martins Junior, D. De Jesus Damiao, T. Martins, M.E. Pol, M.H.G. Souza

Universidade do Estado do Rio de Janeiro, Rio de Janeiro, Brazil

W.L. Aldá Júnior, W. Carvalho, A. Custódio, E.M. Da Costa, C. De Oliveira Martins, S. Fonseca De Souza, D. Matos Figueiredo, L. Mundim, H. Nogima, V. Oguri, W.L. Prado Da Silva, A. Santoro, S.M. Silva Do Amaral, L. Soares Jorge, A. Sznajder

Instituto de Física Teórica, Universidade Estadual Paulista, Sao Paulo, Brazil

C.A. Bernardes³, F.A. Dias⁴, T.R. Fernandez Perez Tomei, E. M. Gregores³, C. Lagana, F. Marinho, P.G. Mercadante³, S.F. Novaes, Sandra S. Padula

Institute for Nuclear Research and Nuclear Energy, Sofia, Bulgaria

V. Genchev¹, P. Iaydjiev¹, S. Piperov, M. Rodozov, S. Stoykova, G. Sultanov, V. Tcholakov, R. Trayanov, M. Vutova

University of Sofia, Sofia, Bulgaria

A. Dimitrov, R. Hadjiiska, V. Kozhuharov, L. Litov, B. Pavlov, P. Petkov

Institute of High Energy Physics, Beijing, China

J.G. Bian, G.M. Chen, H.S. Chen, C.H. Jiang, D. Liang, S. Liang, X. Meng, J. Tao, J. Wang, X. Wang, Z. Wang, H. Xiao, M. Xu, J. Zang, Z. Zhang

State Key Lab. of Nucl. Phys. and Tech., Peking University, Beijing, China

C. Asawatangtrakuldee, Y. Ban, S. Guo, Y. Guo, W. Li, S. Liu, Y. Mao, S.J. Qian, H. Teng, S. Wang, B. Zhu, W. Zou

Universidad de Los Andes, Bogota, Colombia

C. Avila, B. Gomez Moreno, A.F. Osorio Oliveros, J.C. Sanabria

Technical University of Split, Split, Croatia

N. Godinovic, D. Lelas, R. Plestina⁵, D. Polic, I. Puljak¹

University of Split, Split, Croatia

Z. Antunovic, M. Kovac

Institute Rudjer Boskovic, Zagreb, Croatia

V. Brigljevic, S. Duric, K. Kadija, J. Luetic, S. Morovic

University of Cyprus, Nicosia, Cyprus

A. Attikis, M. Galanti, G. Mavromanolakis, J. Mousa, C. Nicolaou, F. Ptochos, P.A. Razis

Charles University, Prague, Czech Republic

M. Finger, M. Finger Jr.

Academy of Scientific Research and Technology of the Arab Republic of Egypt, Egyptian Network of High Energy Physics, Cairo, Egypt

Y. Assran⁶, S. Elgammal⁷, A. Ellithi Kamel⁸, S. Khalil⁷, M.A. Mahmoud⁹, A. Radi^{10,11}

National Institute of Chemical Physics and Biophysics, Tallinn, Estonia

M. Kadastik, M. Müntel, M. Raidal, L. Rebane, A. Tiko

Department of Physics, University of Helsinki, Helsinki, Finland

V. Azzolini, P. Eerola, G. Fedi, M. Voutilainen

Helsinki Institute of Physics, Helsinki, Finland

J. Härkönen, A. Heikkinen, V. Karimäki, R. Kinnunen, M.J. Kortelainen, T. Lampén, K. Lassila-Perini, S. Lehti, T. Lindén, P. Luukka, T. Mäenpää, T. Peltola, E. Tuominen, J. Tuominiemi, E. Tuovinen, D. Ungaro, L. Wendland

Lappeenranta University of Technology, Lappeenranta, Finland

K. Banzuzi, A. Korpela, T. Tuuva

DSM/IRFU, CEA/Saclay, Gif-sur-Yvette, France

M. Besancon, S. Choudhury, M. Dejjardin, D. Denegri, B. Fabbro, J.L. Faure, F. Ferri, S. Ganjour, A. Givernaud, P. Gras, G. Hamel de Monchenault, P. Jarry, E. Locci, J. Malcles, L. Millischer, A. Nayak, J. Rander, A. Rosowsky, I. Shreyber, M. Titov

Laboratoire Leprince-Ringuet, Ecole Polytechnique, IN2P3-CNRS, Palaiseau, France

S. Baffioni, F. Beaudette, L. Benhabib, L. Bianchini, M. Bluj¹², C. Broutin, P. Busson, C. Charlot, N. Daci, T. Dahms, L. Dobrzynski, R. Granier de Cassagnac, M. Haguenaer, P. Miné, C. Mironov, C. Ochando, P. Paganini, D. Sabes, R. Salerno, Y. Sirois, C. Veelken, A. Zabi

Institut Pluridisciplinaire Hubert Curien, Université de Strasbourg, Université de Haute Alsace Mulhouse, CNRS/IN2P3, Strasbourg, France

J.-L. Agram¹³, J. Andrea, D. Bloch, D. Bodin, J.-M. Brom, M. Cardaci, E.C. Chabert, C. Collard, E. Conte¹³, F. Drouhin¹³, C. Ferro, J.-C. Fontaine¹³, D. Gelé, U. Goerlach, P. Juillot, M. Karim¹³, A.-C. Le Bihan, P. Van Hove

Centre de Calcul de l'Institut National de Physique Nucleaire et de Physique des Particules (IN2P3), Villeurbanne, France

F. Fassi, D. Mercier

Université de Lyon, Université Claude Bernard Lyon 1, CNRS-IN2P3, Institut de Physique Nucléaire de Lyon, Villeurbanne, France

S. Beauceron, N. Beaupere, O. Bondu, G. Boudoul, H. Brun, J. Chasserat, R. Chierici¹, D. Contardo, P. Depasse, H. El Mamouni, J. Fay, S. Gascon, M. Gouzevitch, B. Ille, T. Kurca, M. Lethuillier, L. Mirabito, S. Perries, V. Sordini, S. Tosi, Y. Tschudi, P. Verdier, S. Viret

Institute of High Energy Physics and Informatization, Tbilisi State University, Tbilisi, Georgia

Z. Tsamalaidze¹⁴

RWTH Aachen University, I. Physikalisches Institut, Aachen, Germany

G. Anagnostou, S. Beranek, M. Edelhoff, L. Feld, N. Heracleous, O. Hindrichs, R. Jussen, K. Klein, J. Merz, A. Ostapchuk, A. Perieanu, F. Raupach, J. Sammet, S. Schael, D. Sprenger, H. Weber, B. Wittmer, V. Zhukov¹⁵

RWTH Aachen University, III. Physikalisches Institut A, Aachen, Germany

M. Ata, J. Caudron, E. Dietz-Laursonn, M. Erdmann, A. Güth, T. Hebbeker, C. Heidemann, K. Hoepfner, D. Klingebiel, P. Kreuzer, J. Lingemann, C. Magass, M. Merschmeyer, A. Meyer, M. Olschewski, P. Papacz, H. Pieta, H. Reithler, S.A. Schmitz, L. Sonnenschein, J. Steggemann, D. Teyssier, M. Weber

RWTH Aachen University, III. Physikalisches Institut B, Aachen, Germany

M. Bontenackels, V. Cherepanov, M. Davids, G. Flügge, H. Geenen, M. Geisler, W. Haj Ahmad, F. Hoehle, B. Kargoll, T. Kress, Y. Kuessel, A. Linn, A. Nowack, L. Perchalla, O. Pooth, J. Rennefeld, P. Sauerland, A. Stahl

Deutsches Elektronen-Synchrotron, Hamburg, Germany

M. Aldaya Martin, J. Behr, W. Behrenhoff, U. Behrens, M. Bergholz¹⁶, A. Bethani, K. Borrás, A. Burgmeier, A. Cakir, L. Calligaris, A. Campbell, E. Castro, F. Costanza, D. Dammann, G. Eckerlin, D. Eckstein, D. Fischer, G. Flucke, A. Geiser, I. Glushkov, S. Habib, J. Hauk, H. Jung¹, M. Kasemann, P. Katsas, C. Kleinwort, H. Kluge, A. Knutsson, M. Krämer, D. Krücker, E. Kuznetsova, W. Lange, W. Lohmann¹⁶, B. Lutz, R. Mankel, I. Marfin, M. Marienfeld, I.-A. Melzer-Pellmann, A.B. Meyer, J. Mnich, A. Mussgiller, S. Naumann-Emme, J. Olzem, H. Perrey, A. Petrukhin, D. Pitzl, A. Raspereza, P.M. Ribeiro Cipriano, C. Riedl, M. Rosin, J. Salfeld-Nebgen, R. Schmidt¹⁶, T. Schoerner-Sadenius, N. Sen, A. Spiridonov, M. Stein, R. Walsh, C. Wissing

University of Hamburg, Hamburg, Germany

C. Autermann, V. Blobel, S. Bobrovskiy, J. Draeger, H. Enderle, J. Erfle, U. Gebbert, M. Görner, T. Hermanns, R.S. Höing, K. Kaschube, G. Kaussen, H. Kirschenmann, R. Klanner, J. Lange, B. Mura, F. Nowak, N. Pietsch, C. Sander, H. Schettler, P. Schleper, E. Schlieckau, A. Schmidt, M. Schröder, T. Schum, H. Stadie, G. Steinbrück, J. Thomsen

Institut für Experimentelle Kernphysik, Karlsruhe, Germany

C. Barth, J. Berger, T. Chwalek, W. De Boer, A. Dierlamm, M. Feindt, M. Guthoff¹, C. Hackstein, F. Hartmann, M. Heinrich, H. Held, K.H. Hoffmann, S. Honc, I. Katkov¹⁵, J.R. Komaragiri, D. Martschei, S. Mueller, Th. Müller, M. Niegel, A. Nürnberg, O. Oberst, A. Oehler, J. Ott, T. Peiffer, G. Quast, K. Rabbertz, F. Ratnikov, N. Ratnikova, S. Röcker, C. Saout, A. Scheurer, F.-P. Schilling, M. Schmanau, G. Schott, H.J. Simonis, F.M. Stober, D. Troendle, R. Ulrich, J. Wagner-Kuhr, T. Weiler, M. Zeise, E.B. Ziebarth

Institute of Nuclear Physics "Demokritos", Aghia Paraskevi, Greece

G. Daskalakis, T. Gerasis, S. Kesisoglou, A. Kyriakis, D. Loukas, I. Manolakos, A. Markou, C. Markou, C. Mavrommatis, E. Ntomari

University of Athens, Athens, Greece

L. Gouskos, T.J. Mertzimekis, A. Panagiotou, N. Saoulidou

University of Ioánnina, Ioánnina, Greece

I. Evangelou, C. Foudas¹, P. Kokkas, N. Manthos, I. Papadopoulos, V. Patras

KFKI Research Institute for Particle and Nuclear Physics, Budapest, Hungary

G. Bencze, C. Hajdu¹, P. Hidas, D. Horvath¹⁷, K. Krajczar¹⁸, B. Radics, F. Sikler¹, V. Veszpremi, G. Vesztergombi¹⁸

Institute of Nuclear Research ATOMKI, Debrecen, Hungary

N. Beni, S. Czellar, J. Molnar, J. Palinkas, Z. Szillasi

University of Debrecen, Debrecen, Hungary

J. Karancsi, P. Raics, Z.L. Trocsanyi, B. Ujvari

Panjab University, Chandigarh, India

S.B. Beri, V. Bhatnagar, N. Dhingra, R. Gupta, M. Jindal, M. Kaur, J.M. Kohli, M.Z. Mehta, N. Nishu, L.K. Saini, A. Sharma, J. Singh

University of Delhi, Delhi, India

S. Ahuja, A. Bhardwaj, B.C. Choudhary, A. Kumar, A. Kumar, S. Malhotra, M. Naimuddin, K. Ranjan, V. Sharma, R.K. Shivpuri

Saha Institute of Nuclear Physics, Kolkata, India

S. Banerjee, S. Bhattacharya, S. Dutta, B. Gomber, Sa. Jain, Sh. Jain, R. Khurana, S. Sarkar

Bhabha Atomic Research Centre, Mumbai, India

A. Abdulsalam, R.K. Choudhury, D. Dutta, S. Kailas, V. Kumar, P. Mehta, A.K. Mohanty¹, L.M. Pant, P. Shukla

Tata Institute of Fundamental Research - EHEP, Mumbai, India

T. Aziz, S. Ganguly, M. Guchait¹⁹, M. Maity²⁰, G. Majumder, K. Mazumdar, G.B. Mohanty, B. Parida, K. Sudhakar, N. Wickramage

Tata Institute of Fundamental Research - HECR, Mumbai, India

S. Banerjee, S. Dugad

Institute for Research in Fundamental Sciences (IPM), Tehran, Iran

H. Arfaei, H. Bakhshiansohi²¹, S.M. Etesami²², A. Fahim²¹, M. Hashemi, H. Hesari, A. Jafari²¹, M. Khakzad, A. Mohammadi²³, M. Mohammadi Najafabadi, S. Paktinat Mehdiabadi, B. Safarzadeh²⁴, M. Zeinali²²

INFN Sezione di Bari ^a, Università di Bari ^b, Politecnico di Bari ^c, Bari, Italy

M. Abbrescia^{a,b}, L. Barbone^{a,b}, C. Calabria^{a,b,1}, S.S. Chhibra^{a,b}, A. Colaleo^a, D. Creanza^{a,c}, N. De Filippis^{a,c,1}, M. De Palma^{a,b}, L. Fiore^a, G. Iaselli^{a,c}, L. Lusito^{a,b}, G. Maggi^{a,c}, M. Maggi^a, B. Marangelli^{a,b}, S. My^{a,c}, S. Nuzzo^{a,b}, N. Pacifico^{a,b}, A. Pompili^{a,b}, G. Pugliese^{a,c}, G. Selvaggi^{a,b}, L. Silvestris^a, G. Singh^{a,b}, G. Zito^a

INFN Sezione di Bologna ^a, Università di Bologna ^b, Bologna, Italy

G. Abbiendi^a, A.C. Benvenuti^a, D. Bonacorsi^{a,b}, S. Braibant-Giacomelli^{a,b}, L. Brigliadori^{a,b}, P. Capiluppi^{a,b}, A. Castro^{a,b}, F.R. Cavallo^a, M. Cuffiani^{a,b}, G.M. Dallavalle^a, F. Fabbri^a, A. Fanfani^{a,b}, D. Fasanella^{a,b,1}, P. Giacomelli^a, C. Grandi^a, L. Guiducci, S. Marcellini^a, G. Masetti^a, M. Meneghelli^{a,b,1}, A. Montanari^a, F.L. Navarria^{a,b}, F. Odorici^a, A. Perrotta^a, F. Primavera^{a,b}, A.M. Rossi^{a,b}, T. Rovelli^{a,b}, G. Siroli^{a,b}, R. Travaglini^{a,b}

INFN Sezione di Catania ^a, Università di Catania ^b, Catania, Italy

S. Albergo^{a,b}, G. Cappello^{a,b}, M. Chiorboli^{a,b}, S. Costa^{a,b}, R. Potenza^{a,b}, A. Tricomi^{a,b}, C. Tuve^{a,b}

INFN Sezione di Firenze ^a, Università di Firenze ^b, Firenze, Italy

G. Barbagli^a, V. Ciulli^{a,b}, C. Civinini^a, R. D'Alessandro^{a,b}, E. Focardi^{a,b}, S. Frosali^{a,b}, E. Gallo^a, S. Gonzi^{a,b}, M. Meschini^a, S. Paoletti^a, G. Sguazzoni^a, A. Tropiano^{a,1}

INFN Laboratori Nazionali di Frascati, Frascati, Italy

L. Benussi, S. Bianco, S. Colafranceschi²⁵, F. Fabbri, D. Piccolo

INFN Sezione di Genova, Genova, Italy

P. Fabbriatore, R. Musenich

INFN Sezione di Milano-Bicocca ^a, Università di Milano-Bicocca ^b, Milano, Italy

A. Benaglia^{a,b,1}, F. De Guio^{a,b}, L. Di Matteo^{a,b,1}, S. Fiorendi^{a,b}, S. Gennai^{a,1}, A. Ghezzi^{a,b}, S. Malvezzi^a, R.A. Manzoni^{a,b}, A. Martelli^{a,b}, A. Massironi^{a,b,1}, D. Menasce^a, L. Moroni^a, M. Paganoni^{a,b}, D. Pedrini^a, S. Ragazzi^{a,b}, N. Redaelli^a, S. Sala^a, T. Tabarelli de Fatis^{a,b}

INFN Sezione di Napoli ^a, Università di Napoli "Federico II" ^b, Napoli, Italy

S. Buontempo^a, C.A. Carrillo Montoya^{a,1}, N. Cavallo^{a,26}, A. De Cosa^{a,b,1}, O. Dogangun^{a,b}, F. Fabozzi^{a,26}, A.O.M. Iorio^{a,1}, L. Lista^a, S. Meola^{a,27}, M. Merola^{a,b}, P. Paolucci^{a,1}

INFN Sezione di Padova ^a, Università di Padova ^b, Università di Trento (Trento) ^c, Padova, Italy

P. Azzi^a, N. Bacchetta^{a,1}, D. Bisello^{a,b}, A. Branca^{a,1}, P. Checchia^a, T. Dorigo^a, U. Dosselli^a, F. Gasparini^{a,b}, U. Gasparini^{a,b}, A. Gozzelino^a, K. Kanishchev^{a,c}, S. Lacaprara^a, I. Lazzizzera^{a,c}, M. Margoni^{a,b}, A.T. Meneguzzo^{a,b}, M. Nespolo^{a,1}, L. Perrozzi^a, N. Pozzobon^{a,b}, P. Ronchese^{a,b}, F. Simonetto^{a,b}, E. Torassa^a, M. Tosi^{a,b,1}, S. Vanini^{a,b}, P. Zotto^{a,b}, G. Zumerle^{a,b}

INFN Sezione di Pavia ^a, Università di Pavia ^b, Pavia, Italy

M. Gabusi^{a,b}, S.P. Ratti^{a,b}, C. Riccardi^{a,b}, P. Torre^{a,b}, P. Vitulo^{a,b}

INFN Sezione di Perugia ^a, Università di Perugia ^b, Perugia, Italy

M. Biasini^{a,b}, G.M. Bilei^a, L. Fanò^{a,b}, P. Lariccia^{a,b}, A. Lucaroni^{a,b,1}, G. Mantovani^{a,b}, M. Menichelli^a, A. Nappi^{a,b}, F. Romeo^{a,b}, A. Saha, A. Santocchia^{a,b}, S. Taroni^{a,b,1}

INFN Sezione di Pisa ^a, Università di Pisa ^b, Scuola Normale Superiore di Pisa ^c, Pisa, Italy

P. Azzurri^{a,c}, G. Bagliesi^a, T. Boccali^a, G. Broccolo^{a,c}, R. Castaldi^a, R.T. D'Agnolo^{a,c}, R. Dell'Orso^a, F. Fiori^{a,b,1}, L. Foà^{a,c}, A. Giassi^a, A. Kraan^a, F. Ligabue^{a,c}, T. Lomtadze^a, L. Martini^{a,28}, A. Messineo^{a,b}, F. Palla^a, F. Palmonari^a, A. Rizzi^{a,b}, A.T. Serban^{a,29}, P. Spagnolo^a, P. Squillacioti^{a,1}, R. Tenchini^a, G. Tonelli^{a,b,1}, A. Venturi^{a,1}, P.G. Verdini^a

INFN Sezione di Roma ^a, Università di Roma "La Sapienza" ^b, Roma, Italy

L. Barone^{a,b}, F. Cavallari^a, D. Del Re^{a,b,1}, M. Diemoz^a, M. Grassi^{a,b,1}, E. Longo^{a,b}, P. Meridiani^{a,1}, F. Micheli^{a,b}, S. Nourbakhsh^{a,b}, G. Organtini^{a,b}, R. Paramatti^a, S. Rahatlou^{a,b}, M. Sigamani^a, L. Soffi^{a,b}

INFN Sezione di Torino ^a, Università di Torino ^b, Università del Piemonte Orientale (Novara) ^c, Torino, Italy

N. Amapane^{a,b}, R. Arcidiacono^{a,c}, S. Argiro^{a,b}, M. Arneodo^{a,c}, C. Biino^a, C. Botta^{a,b}, N. Cartiglia^a, M. Costa^{a,b}, N. Demaria^a, A. Graziano^{a,b}, C. Mariotti^{a,1}, S. Maselli^a, E. Migliore^{a,b}, V. Monaco^{a,b}, M. Musich^{a,1}, M.M. Obertino^{a,c}, N. Pastrone^a, M. Pelliccioni^a, A. Potenza^{a,b}, A. Romero^{a,b}, M. Ruspa^{a,c}, R. Sacchi^{a,b}, A. Solano^{a,b}, A. Staiano^a, A. Vilela Pereira^a, L. Visca^{a,b}

INFN Sezione di Trieste ^a, Università di Trieste ^b, Trieste, Italy

S. Belforte^a, F. Cossutti^a, G. Della Ricca^{a,b}, B. Gobbo^a, M. Marone^{a,b,1}, D. Montanino^{a,b,1}, A. Penzo^a, A. Schizzi^{a,b}

Kangwon National University, Chunchon, Korea

S.G. Heo, T.Y. Kim, S.K. Nam

Kyungpook National University, Daegu, Korea

S. Chang, J. Chung, D.H. Kim, G.N. Kim, D.J. Kong, H. Park, S.R. Ro, D.C. Son, T. Son

Chonnam National University, Institute for Universe and Elementary Particles, Kwangju, Korea

J.Y. Kim, Zero J. Kim, S. Song

Konkuk University, Seoul, Korea

H.Y. Jo

Korea University, Seoul, Korea

S. Choi, D. Gyun, B. Hong, M. Jo, H. Kim, T.J. Kim, K.S. Lee, D.H. Moon, S.K. Park, E. Seo

University of Seoul, Seoul, Korea

M. Choi, S. Kang, H. Kim, J.H. Kim, C. Park, I.C. Park, S. Park, G. Ryu

Sungkyunkwan University, Suwon, Korea

Y. Cho, Y. Choi, Y.K. Choi, J. Goh, M.S. Kim, E. Kwon, B. Lee, J. Lee, S. Lee, H. Seo, I. Yu

Vilnius University, Vilnius, Lithuania

M.J. Bilinskas, I. Grigelionis, M. Janulis, A. Juodagalvis

Centro de Investigacion y de Estudios Avanzados del IPN, Mexico City, Mexico

H. Castilla-Valdez, E. De La Cruz-Burelo, I. Heredia-de La Cruz, R. Lopez-Fernandez, R. Magaña Villalba, J. Martínez-Ortega, A. Sánchez-Hernández, L.M. Villasenor-Cendejas

Universidad Iberoamericana, Mexico City, Mexico

S. Carrillo Moreno, F. Vazquez Valencia

Benemerita Universidad Autonoma de Puebla, Puebla, Mexico

H.A. Salazar Ibarguen

Universidad Autónoma de San Luis Potosí, San Luis Potosí, Mexico

E. Casimiro Linares, A. Morelos Pineda, M.A. Reyes-Santos

University of Auckland, Auckland, New Zealand

D. Krofcheck, C.H. Yiu

University of Canterbury, Christchurch, New Zealand

A.J. Bell, P.H. Butler, R. Doesburg, S. Reucroft, H. Silverwood

National Centre for Physics, Quaid-I-Azam University, Islamabad, Pakistan

M. Ahmad, M.I. Asghar, H.R. Hoorani, S. Khalid, W.A. Khan, T. Khurshid, S. Qazi, M.A. Shah, M. Shoaib

Institute of Experimental Physics, Faculty of Physics, University of Warsaw, Warsaw, Poland

G. Brona, K. Bunkowski, M. Cwiok, W. Dominik, K. Doroba, A. Kalinowski, M. Konecki, J. Krolikowski

Soltan Institute for Nuclear Studies, Warsaw, Poland

H. Bialkowska, B. Boimska, T. Frueboes, R. Gokieli, M. Górski, M. Kazana, K. Nawrocki, K. Romanowska-Rybinska, M. Szleper, G. Wrochna, P. Zalewski

Laboratório de Instrumentação e Física Experimental de Partículas, Lisboa, Portugal

N. Almeida, P. Bargassa, A. David, P. Faccioli, P.G. Ferreira Parracho, M. Gallinaro, J. Seixas, J. Varela, P. Vischia

Joint Institute for Nuclear Research, Dubna, Russia

S. Afanasiev, I. Belotelov, P. Bunin, I. Golutvin, I. Gorbunov, A. Kamenev, V. Karjavin, G. Kozlov, A. Lanev, A. Malakhov, P. Moisenz, V. Palichik, V. Perelygin, S. Shmatov, V. Smirnov, A. Volodko, A. Zarubin

Petersburg Nuclear Physics Institute, Gatchina (St Petersburg), Russia

S. Evstyukhin, V. Golovtsov, Y. Ivanov, V. Kim, P. Levchenko, V. Murzin, V. Oreshkin, I. Smirnov, V. Sulimov, L. Uvarov, S. Vavilov, A. Vorobyev, An. Vorobyev

Institute for Nuclear Research, Moscow, Russia

Yu. Andreev, A. Dermenev, S. Gninenko, N. Golubev, M. Kirsanov, N. Krasnikov, V. Matveev, A. Pashenkov, D. Tlisov, A. Toropin

Institute for Theoretical and Experimental Physics, Moscow, Russia

V. Epshteyn, M. Erofeeva, V. Gavrilov, M. Kossov¹, N. Lychkovskaya, V. Popov, G. Safronov, S. Semenov, V. Stolin, E. Vlasov, A. Zhokin

Moscow State University, Moscow, Russia

A. Belyaev, E. Boos, A. Ershov, A. Gribushin, V. Klyukhin, O. Kodolova, V. Korotkikh, I. Lokhtin, A. Markina, S. Obraztsov, M. Perfilov, S. Petrushanko, A. Popov, L. Sarycheva[†], V. Savrin, A. Snigirev, I. Vardanyan

P.N. Lebedev Physical Institute, Moscow, Russia

V. Andreev, M. Azarkin, I. Dremin, M. Kirakosyan, A. Leonidov, G. Mesyats, S.V. Rusakov, A. Vinogradov

State Research Center of Russian Federation, Institute for High Energy Physics, Protvino, Russia

I. Azhgirey, I. Bayshev, S. Bitioukov, V. Grishin¹, V. Kachanov, D. Konstantinov, A. Korablev, V. Krychkin, V. Petrov, R. Ryutin, A. Sobol, L. Tourtchanovitch, S. Troshin, N. Tyurin, A. Uzunian, A. Volkov

University of Belgrade, Faculty of Physics and Vinca Institute of Nuclear Sciences, Belgrade, Serbia

P. Adzic³⁰, M. Djordjevic, M. Ekmedzic, D. Krpic³⁰, J. Milosevic

Centro de Investigaciones Energéticas Medioambientales y Tecnológicas (CIEMAT), Madrid, Spain

M. Aguilar-Benitez, J. Alcaraz Maestre, P. Arce, C. Battilana, E. Calvo, M. Cerrada, M. Chamizo Llatas, N. Colino, B. De La Cruz, A. Delgado Peris, C. Diez Pardos, D. Domínguez Vázquez, C. Fernandez Bedoya, J.P. Fernández Ramos, A. Ferrando, J. Flix, M.C. Fouz, P. Garcia-Abia, O. Gonzalez Lopez, S. Goy Lopez, J.M. Hernandez, M.I. Josa, G. Merino, J. Puerta Pelayo, A. Quintario Olmeda, I. Redondo, L. Romero, J. Santaolalla, M.S. Soares, C. Willmott

Universidad Autónoma de Madrid, Madrid, Spain

C. Albajar, G. Codispoti, J.F. de Trocóniz

Universidad de Oviedo, Oviedo, Spain

J. Cuevas, J. Fernandez Menendez, S. Folgueras, I. Gonzalez Caballero, L. Lloret Iglesias, J. Piedra Gomez³¹

Instituto de Física de Cantabria (IFCA), CSIC-Universidad de Cantabria, Santander, Spain

J.A. Brochero Cifuentes, I.J. Cabrillo, A. Calderon, S.H. Chuang, J. Duarte Campderros, M. Felcini³², M. Fernandez, G. Gomez, J. Gonzalez Sanchez, C. Jorda, P. Lobelle Pardo, A. Lopez Virto, J. Marco, R. Marco, C. Martinez Rivero, F. Matorras, F.J. Munoz Sanchez, T. Rodrigo, A.Y. Rodríguez-Marrero, A. Ruiz-Jimeno, L. Scodellaro, M. Sobron Sanudo, I. Vila, R. Vilar Cortabitarte

CERN, European Organization for Nuclear Research, Geneva, Switzerland

D. Abbaneo, E. Auffray, G. Auzinger, P. Baillon, A.H. Ball, D. Barney, C. Bernet⁵, G. Bianchi, P. Bloch, A. Bocci, A. Bonato, H. Breuker, T. Camporesi, G. Cerminara, T. Christiansen, J.A. Coarasa Perez, D. D'Enterria, A. Dabrowski, A. De Roeck, S. Di Guida, M. Dobson, N. Dupont-Sagorin, A. Elliott-Peisert, B. Frisch, W. Funk, G. Georgiou, M. Giffels, D. Gigi, K. Gill, D. Giordano, M. Giunta, F. Glege, R. Gomez-Reino Garrido, P. Govoni, S. Gowdy, R. Guida, M. Hansen, P. Harris, C. Hartl, J. Harvey, B. Hegner, A. Hinzmann, V. Innocente, P. Janot, K. Kaadze, E. Karavakis, K. Kousouris, P. Lecoq, Y.-J. Lee, P. Lenzi, C. Lourenço, T. Mäki, M. Malberti, L. Malgeri, M. Mannelli, L. Masetti, F. Meijers, S. Mersi, E. Meschi, R. Moser, M.U. Mozer, M. Mulders, P. Musella, E. Nesvold, M. Nguyen, T. Orimoto, L. Orsini, E. Palencia Cortezon, E. Perez, A. Petrilli, A. Pfeiffer, M. Pierini, M. Pimiä, D. Piparo, G. Polese, L. Quertenmont, A. Racz, W. Reece, J. Rodrigues Antunes, G. Rolandi³³, T. Rommerskirchen, C. Rovelli³⁴, M. Rovere, H. Sakulin, F. Santanastasio, C. Schäfer, C. Schwick, I. Segoni, S. Sekmen, A. Sharma, P. Siegrist, P. Silva, M. Simon, P. Sphicas³⁵, D. Spiga, M. Spiropulu⁴, M. Stoye, A. Tsirou, G.I. Veres¹⁸, J.R. Vlimant, H.K. Wöhri, S.D. Worm³⁶, W.D. Zeuner

Paul Scherrer Institut, Villigen, Switzerland

W. Bertl, K. Deiters, W. Erdmann, K. Gabathuler, R. Horisberger, Q. Ingram, H.C. Kaestli, S. König, D. Kotlinski, U. Langenegger, F. Meier, D. Renker, T. Rohe, J. Sibille³⁷

Institute for Particle Physics, ETH Zurich, Zurich, Switzerland

L. Bäni, P. Bortignon, M.A. Buchmann, B. Casal, N. Chanon, Z. Chen, A. Deisher, G. Dissertori, M. Dittmar, M. Dünser, J. Eugster, K. Freudenreich, C. Grab, D. Hits, P. Lecomte, W. Lustermann, P. Martinez Ruiz del Arbol, N. Mohr, F. Moortgat, C. Nägeli³⁸, P. Nef, F. Nessi-Tedaldi, F. Pandolfi, L. Pape, F. Pauss, M. Peruzzi, F.J. Ronga, M. Rossini, L. Sala, A.K. Sanchez, A. Starodumov³⁹, B. Stieger, M. Takahashi, L. Tauscher[†], A. Thea, K. Theofilatos, D. Treille, C. Urscheler, R. Wallny, H.A. Weber, L. Wehrli

Universität Zürich, Zurich, Switzerland

E. Aguilo, C. AMSler, V. Chiochia, S. De Visscher, C. Favaro, M. Ivova Rikova, B. Millan Mejias, P. Otiougova, P. Robmann, H. Snoek, S. Tuppiti, M. Verzetti

National Central University, Chung-Li, Taiwan

Y.H. Chang, K.H. Chen, C.M. Kuo, S.W. Li, W. Lin, Z.K. Liu, Y.J. Lu, D. Mekterovic, A.P. Singh, R. Volpe, S.S. Yu

National Taiwan University (NTU), Taipei, Taiwan

P. Bartalini, P. Chang, Y.H. Chang, Y.W. Chang, Y. Chao, K.F. Chen, C. Dietz, U. Grundler, W.-S. Hou, Y. Hsiung, K.Y. Kao, Y.J. Lei, R.-S. Lu, D. Majumder, E. Petrakou, X. Shi, J.G. Shiu, Y.M. Tzeng, M. Wang

Cukurova University, Adana, Turkey

A. Adiguzel, M.N. Bakirci⁴⁰, S. Cerci⁴¹, C. Dozen, I. Dumanoglu, E. Eskut, S. Girgis, G. Gokbulut, E. Gurpinar, I. Hos, E.E. Kangal, G. Karapinar, A. Kayis Topaksu, G. Onengut, K. Ozdemir, S. Ozturk⁴², A. Polatoz, K. Sogut⁴³, D. Sunar Cerci⁴¹, B. Tali⁴¹, H. Topakli⁴⁰, L.N. Vergili, M. Vergili

Middle East Technical University, Physics Department, Ankara, Turkey

I.V. Akin, T. Aliev, B. Bilin, S. Bilmis, M. Deniz, H. Gamsizkan, A.M. Guler, K. Ocalan, A. Ozpineci, M. Serin, R. Sever, U.E. Surat, M. Yalvac, E. Yildirim, M. Zeyrek

Bogazici University, Istanbul, Turkey

E. Gülmez, B. Isildak⁴⁴, M. Kaya⁴⁵, O. Kaya⁴⁵, S. Ozkorucuklu⁴⁶, N. Sonmez⁴⁷

Istanbul Technical University, Istanbul, Turkey

K. Cankocak

National Scientific Center, Kharkov Institute of Physics and Technology, Kharkov, Ukraine

L. Levchuk

University of Bristol, Bristol, United Kingdom

F. Bostock, J.J. Brooke, E. Clement, D. Cussans, H. Flacher, R. Frazier, J. Goldstein, M. Grimes, G.P. Heath, H.F. Heath, L. Kreczko, S. Metson, D.M. Newbold³⁶, K. Nirunpong, A. Poll, S. Senkin, V.J. Smith, T. Williams

Rutherford Appleton Laboratory, Didcot, United Kingdom

L. Basso⁴⁸, A. Belyaev⁴⁸, C. Brew, R.M. Brown, D.J.A. Cockerill, J.A. Coughlan, K. Harder, S. Harper, J. Jackson, B.W. Kennedy, E. Olaiya, D. Petyt, B.C. Radburn-Smith, C.H. Shepherd-Themistocleous, I.R. Tomalin, W.J. Womersley

Imperial College, London, United Kingdom

R. Bainbridge, G. Ball, R. Beuselinck, O. Buchmuller, D. Colling, N. Cripps, M. Cutajar, P. Dauncey, G. Davies, M. Della Negra, W. Ferguson, J. Fulcher, D. Futyan, A. Gilbert, A. Guneratne Bryer, G. Hall, Z. Hatherell, J. Hays, G. Iles, M. Jarvis, G. Karapostoli, L. Lyons, A.-M. Magnan, J. Marrouche, B. Mathias, R. Nandi, J. Nash, A. Nikitenko³⁹, A. Papageorgiou, J. Pela¹, M. Pesaresi, K. Petridis, M. Pioppi⁴⁹, D.M. Raymond, S. Rogerson, A. Rose, M.J. Ryan, C. Seez, P. Sharp[†], A. Sparrow, A. Tapper, M. Vazquez Acosta, T. Virdee, S. Wakefield, N. Wardle, T. Whyntie

Brunel University, Uxbridge, United Kingdom

M. Barrett, M. Chadwick, J.E. Cole, P.R. Hobson, A. Khan, P. Kyberd, D. Leslie, W. Martin, I.D. Reid, P. Symonds, L. Teodorescu, M. Turner

Baylor University, Waco, USA

K. Hatakeyama, H. Liu, T. Scarborough

The University of Alabama, Tuscaloosa, USA

C. Henderson, P. Rumerio

Boston University, Boston, USA

A. Avetisyan, T. Bose, C. Fantasia, A. Heister, J. St. John, P. Lawson, D. Lazic, J. Rohlf, D. Sperka, L. Sulak

Brown University, Providence, USA

J. Alimena, S. Bhattacharya, D. Cutts, A. Ferapontov, U. Heintz, S. Jabeen, G. Kukartsev, G. Landsberg, M. Luk, M. Narain, D. Nguyen, M. Segala, T. Sinthuprasith, T. Speer, K.V. Tsang

University of California, Davis, Davis, USA

R. Breedon, G. Breto, M. Calderon De La Barca Sanchez, S. Chauhan, M. Chertok, J. Conway, R. Conway, P.T. Cox, J. Dolen, R. Erbacher, M. Gardner, R. Houtz, W. Ko, A. Kopecky, R. Lander, O. Mall, T. Miceli, R. Nelson, D. Pellett, B. Rutherford, M. Searle, J. Smith, M. Squires, M. Tripathi, R. Vasquez Sierra

University of California, Los Angeles, Los Angeles, USA

V. Andreev, D. Cline, R. Cousins, J. Duris, S. Erhan, P. Everaerts, C. Farrell, J. Hauser, M. Ignatenko, C. Plager, G. Rakness, P. Schlein[†], J. Tucker, V. Valuev, M. Weber

University of California, Riverside, Riverside, USA

J. Babb, R. Clare, M.E. Dinardo, J. Ellison, J.W. Gary, F. Giordano, G. Hanson, G.Y. Jeng⁵⁰, H. Liu, O.R. Long, A. Luthra, H. Nguyen, S. Paramesvaran, J. Sturdy, S. Sumowidagdo, R. Wilken, S. Wimpenny

University of California, San Diego, La Jolla, USA

W. Andrews, J.G. Branson, G.B. Cerati, S. Cittolin, D. Evans, F. Golf, A. Holzner, R. Kelley, M. Lebourgeois, J. Letts, I. Macneill, B. Mangano, J. Muelmenstaedt, S. Padhi, C. Palmer, G. Petrucciani, M. Pieri, M. Sani, V. Sharma, S. Simon, E. Sudano, M. Tadel, Y. Tu, A. Vartak, S. Wasserbaech⁵¹, F. Würthwein, A. Yagil, J. Yoo

University of California, Santa Barbara, Santa Barbara, USA

D. Barge, R. Bellan, C. Campagnari, M. D'Alfonso, T. Danielson, K. Flowers, P. Geffert, J. Incandela, C. Justus, P. Kalavase, S.A. Koay, D. Kovalskyi, V. Krutelyov, S. Lowette, N. Mccoll, V. Pavlunin, F. Rebassoo, J. Ribnik, J. Richman, R. Rossin, D. Stuart, W. To, C. West

California Institute of Technology, Pasadena, USA

A. Apresyan, A. Bornheim, Y. Chen, E. Di Marco, J. Duarte, M. Gataullin, Y. Ma, A. Mott, H.B. Newman, C. Rogan, V. Timciuc, P. Traczyk, J. Veverka, R. Wilkinson, Y. Yang, R.Y. Zhu

Carnegie Mellon University, Pittsburgh, USA

B. Akgun, R. Carroll, T. Ferguson, Y. Iiyama, D.W. Jang, Y.F. Liu, M. Paulini, H. Vogel, I. Vorobiev

University of Colorado at Boulder, Boulder, USA

J.P. Cumalat, B.R. Drell, C.J. Edelmaier, W.T. Ford, A. Gaz, B. Heyburn, E. Luiggi Lopez, J.G. Smith, K. Stenson, K.A. Ulmer, S.R. Wagner

Cornell University, Ithaca, USA

L. Agostino, J. Alexander, A. Chatterjee, N. Eggert, L.K. Gibbons, B. Heltsley, W. Hopkins, A. Khukhunaishvili, B. Kreis, N. Mirman, G. Nicolas Kaufman, J.R. Patterson, A. Ryd, E. Salvati, W. Sun, W.D. Teo, J. Thom, J. Thompson, J. Vaughan, Y. Weng, L. Winstrom, P. Wittich

Fairfield University, Fairfield, USA

D. Winn

Fermi National Accelerator Laboratory, Batavia, USA

S. Abdullin, M. Albrow, J. Anderson, L.A.T. Bauerdick, A. Beretvas, J. Berryhill, P.C. Bhat, I. Bloch, K. Burkett, J.N. Butler, V. Chetluru, H.W.K. Cheung, F. Chlebana, V.D. Elvira, I. Fisk, J. Freeman, Y. Gao, D. Green, O. Gutsche, A. Hahn, J. Hanlon, R.M. Harris, J. Hirschauer, B. Hooberman, S. Jindariani, M. Johnson, U. Joshi, B. Kilminster, B. Klima, S. Kunori, S. Kwan, C. Leonidopoulos, D. Lincoln, R. Lipton, L. Lueking, J. Lykken, K. Maeshima, J.M. Marraffino, S. Maruyama, D. Mason, P. McBride, K. Mishra, S. Mrenna, Y. Musienko⁵², C. Newman-Holmes, V. O'Dell, O. Prokofyev, E. Sexton-Kennedy, S. Sharma, W.J. Spalding, L. Spiegel, P. Tan, L. Taylor, S. Tkaczyk, N.V. Tran, L. Uplegger, E.W. Vaandering, R. Vidal, J. Whitmore, W. Wu, F. Yang, F. Yumiceva, J.C. Yun

University of Florida, Gainesville, USA

D. Acosta, P. Avery, D. Bourilkov, M. Chen, S. Das, M. De Gruttola, G.P. Di Giovanni, D. Dobur, A. Drozdetskiy, R.D. Field, M. Fisher, Y. Fu, I.K. Furic, J. Gartner, J. Hugon, B. Kim, J. Konigsberg, A. Korytov, A. Kropivnitskaya, T. Kypreos, J.F. Low, K. Matchev, P. Milenovic⁵³, G. Mitselmakher, L. Muniz, R. Remington, A. Rinkevicius, P. Sellers, N. Skhirtladze, M. Snowball, J. Yelton, M. Zakaria

Florida International University, Miami, USA

V. Gaultney, L.M. Lebolo, S. Linn, P. Markowitz, G. Martinez, J.L. Rodriguez

Florida State University, Tallahassee, USA

T. Adams, A. Askew, J. Bochenek, J. Chen, B. Diamond, S.V. Gleyzer, J. Haas, S. Hagopian, V. Hagopian, M. Jenkins, K.F. Johnson, H. Prosper, V. Veeraraghavan, M. Weinberg

Florida Institute of Technology, Melbourne, USA

M.M. Baarmand, B. Dorney, M. Hohlmann, H. Kalakhety, I. Vodopyanov

University of Illinois at Chicago (UIC), Chicago, USA

M.R. Adams, I.M. Anghel, L. Apanasevich, Y. Bai, V.E. Bazterra, R.R. Betts, I. Bucinskaite, J. Callner, R. Cavanaugh, C. Dragoiu, O. Evdokimov, E.J. Garcia-Solis, L. Gauthier, C.E. Gerber, S. Hamdan, D.J. Hofman, S. Khalatyan, F. Lacroix, M. Malek, C. O'Brien, C. Silkworth, D. Strom, N. Varelas

The University of Iowa, Iowa City, USA

U. Akgun, E.A. Albayrak, B. Bilki⁵⁴, K. Chung, W. Clarida, F. Duru, S. Griffiths, C.K. Lae, J.-P. Merlo, H. Mermerkaya⁵⁵, A. Mestvirishvili, A. Moeller, J. Nachtman, C.R. Newsom, E. Norbeck, J. Olson, Y. Onel, F. Ozok, S. Sen, E. Tiras, J. Wetzel, T. Yetkin, K. Yi

Johns Hopkins University, Baltimore, USA

B.A. Barnett, B. Blumenfeld, S. Bolognesi, D. Fehling, G. Giurgiu, A.V. Gritsan, Z.J. Guo, G. Hu, P. Maksimovic, S. Rappoccio, M. Swartz, A. Whitbeck

The University of Kansas, Lawrence, USA

P. Baringer, A. Bean, G. Benelli, O. Grachov, R.P. Kenny Iii, M. Murray, D. Noonan, S. Sanders, R. Stringer, G. Tinti, J.S. Wood, V. Zhukova

Kansas State University, Manhattan, USA

A.F. Barfuss, T. Bolton, I. Chakaberia, A. Ivanov, S. Khalil, M. Makouski, Y. Maravin, S. Shrestha, I. Svintradze

Lawrence Livermore National Laboratory, Livermore, USA

J. Gronberg, D. Lange, D. Wright

University of Maryland, College Park, USA

A. Baden, M. Boutemour, B. Calvert, S.C. Eno, J.A. Gomez, N.J. Hadley, R.G. Kellogg, M. Kirn, T. Kolberg, Y. Lu, M. Marionneau, A.C. Mignerey, A. Peterman, K. Rossato, A. Skuja, J. Temple, M.B. Tonjes, S.C. Tonwar, E. Twedt

Massachusetts Institute of Technology, Cambridge, USA

G. Bauer, J. Bendavid, W. Busza, E. Butz, I.A. Cali, M. Chan, V. Dutta, G. Gomez Ceballos, M. Goncharov, K.A. Hahn, Y. Kim, M. Klute, W. Li, P.D. Luckey, T. Ma, S. Nahn, C. Paus, D. Ralph, C. Roland, G. Roland, M. Rudolph, G.S.F. Stephans, F. Stöckli, K. Sumorok, K. Sung, D. Velicanu, E.A. Wenger, R. Wolf, B. Wyslouch, S. Xie, M. Yang, Y. Yilmaz, A.S. Yoon, M. Zanetti

University of Minnesota, Minneapolis, USA

S.I. Cooper, P. Cushman, B. Dahmes, A. De Benedetti, G. Franzoni, A. Gude, J. Haupt, S.C. Kao, K. Klapoetke, Y. Kubota, J. Mans, N. Pastika, R. Rusack, M. Sasseville, A. Singovsky, N. Tambe, J. Turkewitz

University of Mississippi, University, USA

L.M. Cremaldi, R. Kroeger, L. Perera, R. Rahmat, D.A. Sanders

University of Nebraska-Lincoln, Lincoln, USA

E. Avdeeva, K. Bloom, S. Bose, J. Butt, D.R. Claes, A. Dominguez, M. Eads, P. Jindal, J. Keller, I. Kravchenko, J. Lazo-Flores, H. Malbouisson, S. Malik, G.R. Snow

State University of New York at Buffalo, Buffalo, USA

U. Baur, A. Godshalk, I. Iashvili, S. Jain, A. Kharchilava, A. Kumar, S.P. Shipkowski, K. Smith

Northeastern University, Boston, USA

G. Alverson, E. Barberis, D. Baumgartel, M. Chasco, J. Haley, D. Trocino, D. Wood, J. Zhang

Northwestern University, Evanston, USA

A. Anastassov, A. Kubik, N. Mucia, N. Odell, R.A. Ofierzynski, B. Pollack, A. Pozdnyakov, M. Schmitt, S. Stoynev, M. Velasco, S. Won

University of Notre Dame, Notre Dame, USA

L. Antonelli, D. Berry, A. Brinkerhoff, M. Hildreth, C. Jessop, D.J. Karmgard, J. Kolb, K. Lannon, W. Luo, S. Lynch, N. Marinelli, D.M. Morse, T. Pearson, R. Ruchti, J. Slaunwhite, N. Valls, M. Wayne, M. Wolf

The Ohio State University, Columbus, USA

B. Bylsma, L.S. Durkin, C. Hill, R. Hughes, K. Kotov, T.Y. Ling, D. Puigh, M. Rodenburg, C. Vuosalo, G. Williams, B.L. Winer

Princeton University, Princeton, USA

N. Adam, E. Berry, P. Elmer, D. Gerbaudo, V. Halyo, P. Hebda, J. Hegeman, A. Hunt, E. Laird, D. Lopes Pegna, P. Lujan, D. Marlow, T. Medvedeva, M. Mooney, J. Olsen, P. Piroué, X. Quan, A. Raval, H. Saka, D. Stickland, C. Tully, J.S. Werner, A. Zuranski

University of Puerto Rico, Mayaguez, USA

J.G. Acosta, E. Brownson, X.T. Huang, A. Lopez, H. Mendez, S. Oliveros, J.E. Ramirez Vargas, A. Zatserklyaniy

Purdue University, West Lafayette, USA

E. Alagoz, V.E. Barnes, D. Benedetti, G. Bolla, D. Bortoletto, M. De Mattia, A. Everett, Z. Hu,

M. Jones, O. Koybasi, M. Kress, A.T. Laasanen, N. Leonardo, V. Maroussov, P. Merkel, D.H. Miller, N. Neumeister, I. Shipsey, D. Silvers, A. Svyatkovskiy, M. Vidal Marono, H.D. Yoo, J. Zablocki, Y. Zheng

Purdue University Calumet, Hammond, USA

S. Guragain, N. Parashar

Rice University, Houston, USA

A. Adair, C. Boulahouache, V. Cuplov, K.M. Ecklund, F.J.M. Geurts, B.P. Padley, R. Redjimi, J. Roberts, J. Zabel

University of Rochester, Rochester, USA

B. Betchart, A. Bodek, Y.S. Chung, R. Covarelli, P. de Barbaro, R. Demina, Y. Eshaq, A. Garcia-Bellido, P. Goldenzweig, Y. Gotra, J. Han, A. Harel, S. Korjenevski, D.C. Miner, D. Vishnevskiy, M. Zielinski

The Rockefeller University, New York, USA

A. Bhatti, R. Ciesielski, L. Demortier, K. Goulios, G. Lungu, S. Malik, C. Mesropian

Rutgers, the State University of New Jersey, Piscataway, USA

S. Arora, A. Barker, J.P. Chou, C. Contreras-Campana, E. Contreras-Campana, D. Duggan, D. Ferencek, Y. Gershtein, R. Gray, E. Halkiadakis, D. Hidas, A. Lath, S. Panwalkar, M. Park, R. Patel, V. Rekovic, A. Richards, J. Robles, K. Rose, S. Salur, S. Schnetzer, C. Seitz, S. Somalwar, R. Stone, S. Thomas

University of Tennessee, Knoxville, USA

G. Cerizza, M. Hollingsworth, S. Spanier, Z.C. Yang, A. York

Texas A&M University, College Station, USA

R. Eusebi, W. Flanagan, J. Gilmore, T. Kamon⁵⁶, V. Khotilovich, R. Montalvo, I. Osipenkov, Y. Pakhotin, A. Perloff, J. Roe, A. Safonov, T. Sakuma, S. Sengupta, I. Suarez, A. Tatarinov, D. Toback

Texas Tech University, Lubbock, USA

N. Akchurin, J. Damgov, P.R. Duderod, C. Jeong, K. Kovitanggoon, S.W. Lee, T. Libeiro, Y. Roh, I. Volobouev

Vanderbilt University, Nashville, USA

E. Appelt, D. Engh, C. Florez, S. Greene, A. Gurrola, W. Johns, C. Johnston, P. Kurt, C. Maguire, A. Melo, P. Sheldon, B. Snook, S. Tuo, J. Velkovska

University of Virginia, Charlottesville, USA

M.W. Arenton, M. Balazs, S. Boutle, B. Cox, B. Francis, J. Goodell, R. Hirosky, A. Ledovskoy, C. Lin, C. Neu, J. Wood, R. Yohay

Wayne State University, Detroit, USA

S. Gollapinni, R. Harr, P.E. Karchin, C. Kottachchi Kankanamge Don, P. Lamichhane, A. Sakharov

University of Wisconsin, Madison, USA

M. Anderson, M. Bachtis, D. Belknap, L. Borrello, D. Carlsmith, M. Cepeda, S. Dasu, L. Gray, K.S. Grogg, M. Grothe, R. Hall-Wilton, M. Herndon, A. Hervé, P. Klabbers, J. Klukas, A. Lanaro, C. Lazaridis, J. Leonard, R. Loveless, A. Mohapatra, I. Ojalvo, G.A. Pierro, I. Ross, A. Savin, W.H. Smith, J. Swanson

†: Deceased

- 1: Also at CERN, European Organization for Nuclear Research, Geneva, Switzerland
- 2: Also at National Institute of Chemical Physics and Biophysics, Tallinn, Estonia
- 3: Also at Universidade Federal do ABC, Santo Andre, Brazil
- 4: Also at California Institute of Technology, Pasadena, USA
- 5: Also at Laboratoire Leprince-Ringuet, Ecole Polytechnique, IN2P3-CNRS, Palaiseau, France
- 6: Also at Suez Canal University, Suez, Egypt
- 7: Also at Zewail City of Science and Technology, Zewail, Egypt
- 8: Also at Cairo University, Cairo, Egypt
- 9: Also at Fayoum University, El-Fayoum, Egypt
- 10: Also at British University, Cairo, Egypt
- 11: Now at Ain Shams University, Cairo, Egypt
- 12: Also at Soltan Institute for Nuclear Studies, Warsaw, Poland
- 13: Also at Université de Haute-Alsace, Mulhouse, France
- 14: Now at Joint Institute for Nuclear Research, Dubna, Russia
- 15: Also at Moscow State University, Moscow, Russia
- 16: Also at Brandenburg University of Technology, Cottbus, Germany
- 17: Also at Institute of Nuclear Research ATOMKI, Debrecen, Hungary
- 18: Also at Eötvös Loránd University, Budapest, Hungary
- 19: Also at Tata Institute of Fundamental Research - HECR, Mumbai, India
- 20: Also at University of Visva-Bharati, Santiniketan, India
- 21: Also at Sharif University of Technology, Tehran, Iran
- 22: Also at Isfahan University of Technology, Isfahan, Iran
- 23: Also at Shiraz University, Shiraz, Iran
- 24: Also at Plasma Physics Research Center, Science and Research Branch, Islamic Azad University, Teheran, Iran
- 25: Also at Facoltà Ingegneria Università di Roma, Roma, Italy
- 26: Also at Università della Basilicata, Potenza, Italy
- 27: Also at Università degli Studi Guglielmo Marconi, Roma, Italy
- 28: Also at Università degli studi di Siena, Siena, Italy
- 29: Also at University of Bucharest, Faculty of Physics, Bucuresti-Magurele, Romania
- 30: Also at Faculty of Physics of University of Belgrade, Belgrade, Serbia
- 31: Also at University of Florida, Gainesville, USA
- 32: Also at University of California, Los Angeles, Los Angeles, USA
- 33: Also at Scuola Normale e Sezione dell' INFN, Pisa, Italy
- 34: Also at INFN Sezione di Roma; Università di Roma "La Sapienza", Roma, Italy
- 35: Also at University of Athens, Athens, Greece
- 36: Also at Rutherford Appleton Laboratory, Didcot, United Kingdom
- 37: Also at The University of Kansas, Lawrence, USA
- 38: Also at Paul Scherrer Institut, Villigen, Switzerland
- 39: Also at Institute for Theoretical and Experimental Physics, Moscow, Russia
- 40: Also at Gaziosmanpasa University, Tokat, Turkey
- 41: Also at Adiyaman University, Adiyaman, Turkey
- 42: Also at The University of Iowa, Iowa City, USA
- 43: Also at Mersin University, Mersin, Turkey
- 44: Also at Ozyegin University, Istanbul, Turkey
- 45: Also at Kafkas University, Kars, Turkey
- 46: Also at Suleyman Demirel University, Isparta, Turkey
- 47: Also at Ege University, Izmir, Turkey

48: Also at School of Physics and Astronomy, University of Southampton, Southampton, United Kingdom

49: Also at INFN Sezione di Perugia; Università di Perugia, Perugia, Italy

50: Also at University of Sydney, Sydney, Australia

51: Also at Utah Valley University, Orem, USA

52: Also at Institute for Nuclear Research, Moscow, Russia

53: Also at University of Belgrade, Faculty of Physics and Vinca Institute of Nuclear Sciences, Belgrade, Serbia

54: Also at Argonne National Laboratory, Argonne, USA

55: Also at Erzincan University, Erzincan, Turkey

56: Also at Kyungpook National University, Daegu, Korea